FCTUC

Departamento de Física

Faculdade de Ciências e Tecnologia

Universidade de Coimbra

plux

Plux

Engenharia de Biosensores, Lda

Development of a Heart Rate Variability analysis tool

José Miguel Medeiros

Coimbra, 2010

Development of a Heart Rate Variability analysis tool

Coordinator: Prof. Dr. Marco Reis

Advisor at PLUX: Prof. Dr. Hugo Gamboa

Co-Advisor at PLUX: Eng. Susana Palma

Committee:

Prof. Dr. Marco Reis

Prof. Dr. Hugo Gamboa

Prof. Dr. Jorge Landeck

Prof. Dr. Custódio Loureiro

A Thesis submitted for obtaining the degree of Masters

in Biomedical Engineering

Departmento de Física

Faculdade de Ciências e Tecnologia,

Universidade de Coimbra

September 2010

To my family and my friends

for always supporting me...

Acknowledgments

The work I've done over the last year, which is summarized in this thesis, would not have been possible without the support of the people closest to me. So I owe them my deepest gratitude.

I would like to thank, first, to my advisor at *PLUX, Lda*, Prof. Dr. Hugo Gamboa for the unique opportunity offered by accepting me as a trainee and for all the time and knowledge he had shared with me.

I would also like to thank to my advisor at University of Coimbra, Prof. Dr. Marco Reis, who always had the willingness to listen to my questions and for giving me important advice for the development of my work.

Thanks to all my colleagues at *PLUX, Lda* for having received me with open arms and for always being available to help, particularly to Eng. Susana Palma that was the person who most closely followed my work and contributed to it, decisively, allowing it to be carried out successfully.

A special thanks to all my friends who always supported me, especially Rui Martins, that was, besides my partner during this year at *PLUX, Lda*, an amazing friend that always had the patience to listen and help me with my doubts.

Could not fail to thank my girlfriend, Sandra, who was always by my side willing to listen to my problems and uncertainties.

Finally, I would like to thank all my family, especially my parents, my brothers, my grandmother Maria Alice, my aunt Lúcia and my cousins Carolina and Joana, for all the support and motivation they gave me, without whom it would be impossible to overcome all the difficulties and achieve my professional and personal goals.

Abstract

Heart Rate Variability (HRV) concerns the analysis of the phenomenon underlying the variability between consecutive heartbeats. During the last three decades, significant effort has been made to understand its physiological basis and implications in different pathologies. Such studies have revealed, among other aspects, that HRV its a mirror of the control actions exerted by the Autonomic Nervous System (ANS) in the Sinoatrial (SA) node. Since the SA node is responsible for setting the heartbeat, the two branches comprising the ANS, sympathetic and parasympathetic, have a special role in controlling such variability.

The main goals behind this work were: to develop an open source, reliable and easy-to-use Graphical User Interface (GUI) able to perform a complete HRV analysis; to investigate and possibly implement alternative methods to perform an HRV analysis; and also to validate the developments achieved.

As a result of the work carried out, we have manage to develop a cross platform and full featured Python based GUI for HRV computation using the standard procedure based on ECG signals and another alternative methodology based on PPG signals. We have also conducted three different studies in order to analyze the validity of our tool. The first study aimed to validate our HRV GUI and revealed the absence of any significant differences between our GUI and a reference tool. The second study evaluated both specificity and sensitivity of the algorithm that we have developed to detect systolic peaks in PPG signals, where high performance levels were attained. Finally, the third study, aimed to validate the use of PPG signals as an alternative to ECG signals for computing HRV, revealed high levels of correlation between the same parameters computed from ECG and PPG signals acquired simultaneously.

Table of Contents

Bibliography **70**

List of Figures

List of Tables

List of Abbreviations and units

ABP Arterial Blood Pulse

ADC Analog-to-Digital Converter

AEB Atrial Ectopic Beat

ANS Autonomic Nervous System

AV Atrioventricular

BP Blood Pressure

BVP Blood Volume Pulse

CNS Central Nervous System

DAN Diabetic Autonomic Neuropathy

ECG Electrocardiogram

FFT Fast Fourier Transform

GUI Graphical User Interface

HF High Frequency

HR Heart Rate

IDE Integrated Development Environment

IIR Infinite Impulse Response

$\overline{HR}$ Mean Heart Rate

$\mathbf{HR_{60}}$ Time Averaged Heart Rate

HRV Heart Rate Variability

HTML HyperText Markup Language

IR Infrared

ᵢHR Instantaneous Heart Rate

ᵢHRs Instantaneous Heart Rates

LED Light-emitting Diode

LF Low Frequency

PVC Premature Ventricular Contraction

PPG Photoplethysmography

PSD Power Spectral Density

PTT Pulse Transit Time

RCVS Respiratory Cardiovascular System

RSA Respiratory Sinus Arrhythmia

SA Sinoatrial

SSF Slope Sum Function

ULF Ultra Low Frequency

VEB Ventricular Ectopic Beat

VEBs Ventricular Ectopic Beats

VLF Very Low Frequency

VT Ventricular Tachycardia

bpm beats per minute

V Volt

Hz hertz

mV millivolt

ms milliseconds

s seconds

min minutes

n.u. normalized units

Chapter 1

Introduction

The oscillation in the interval between consecutive heartbeats, a phenomenon known as Heart Rate Variability (HRV), is one of the most important markers of the autonomous control of Heart Rate (HR) [6].

The SA node is the main pacemaker of the heart and is responsible, in normal conditions, for setting the heart rhythm. Since it is modulated by the sympathetic and parasympathetic branches of the Autonomic Nervous System (ANS) it was proved that the oscillations that happen in the heartbeats intervals reflect such modulation [8]. Therefore, HRV is seen as a promising quantitative index for such oscillations and consequently as a mirror of the ANS activity and a way to better understand it and its relationship with cardiovascular mortality. Several other diseases, such as Diabetic Autonomic Neuropathy (DAN), have been also identified and associated with HRV [9].

The simple computation of HRV parameters along with the growth of signal processing techniques contributed to popularize and spread the use of HRV in the last decades.

Recognition of HRV potential led us to focus our work on the development of an interactive, easy-to-use and reliable software to derive a wide variety of HRV parameters and to search for new possibilities in this field.

The main goals of this project were to develop and implement algorithms to easily and accurately extract HRV parameters from ECG signals, in a first stage, and from both ECG and Photoplethysmography (PPG) signals, in a second stage, and at the same time built a simple HRV GUI that was able to integrate all the algorithms and perform HRV analysis.

This project was developed at *PLUX-Engenharia de Biosensores, Lda* with the aim to combine all the HRV potential with the already available ECG PLUX sensor and with the PPG PLUX sensor that was being developed, in order to offer an innovative solution for physicians and researchers.

1.1   Thesis Overview

The thesis is organized in seven chapters, as follows.

- **Chapter 1**, the current chapter, highlights the motivations and main objectives of the project, as well as make reference to the publications that were produced as a consequence of the work developed during the project.

- **Chapter 2** provides a theoretical introduction to heart physiology, in particular to heart electrophysiology, given its importance for understanding HRV.

- **Chapter 3** describes in detail the HRV theory, the standards used in HRV analysis and the clinical relevance of such parameter.

- **Chapter 4** introduces the PPG signal as an alternative to extract HRV parameters and discusses its validity and possible applications on our project.

- **Chapter 5** explains in detail the development of a *Python* based HRV analysis tool and its main features.

- **Chapter 6** presents the experimental studies implemented, the results obtained and their discussion.

- **Chapter 7** is the last chapter of the thesis and presents the conclusions taken and possible directions to follow in future work.

1.2   Publications

The results obtained in this project have been submitted to two different conferences. The first article submitted, entitled "Blood Volume Pulse Peak Detector with a Double Adaptive Threshold", where the author was the first author, was accepted for oral

presentation in the 6th International Conference on Technology and Medical Sciences that will take place in October 2010 in Porto, while the second one, entitled "Development of a Blood Volume Pulse Sensor to measure Heart Rate Variability", where the author was one of the co-authors, was accepted for poster presentation in the 7th Ibero-American Congress on Sensors - IBERSENSOR 2010 that will take place in November 2010 in Lisbon. These two publications are included in Appendix A.

Chapter 2

Physiological Concepts

2.1   Heart physiology

In this chapter we provide a physiological contextualization in order to introduce key knowledge about the heart activity, in particular regarding its autonomic regulation, which is on the basis of HRV.

The heart is one of the most important organs of the entire human system since it is responsible for rhythmically pump blood all over the body enabling the transport of vital nutrients and oxygen to the cells. The four chambers that compose the heart (see Figure 2.1) have different roles in this hard and essential task. The chambers from the right side (right atrium and right ventricle) deliver deoxygenated blood, that arrives from the systemic circulation, to the lungs, through the pulmonary circulation, while the chambers from the left side (left atrium and left ventricle) deliver oxygenated blood, coming from the lungs, to the entire body, through the systemic circulation [2].

This vital function is regulated by the Central Nervous System (CNS) and it is accomplished thanks to the work of the cardiac muscle that, when electrically stimulated, makes the heart contract and relax in a synchronized way. The electrical stimulation is made through a complex network of cardiac muscle fibers that conduct a wave of electrical current with a specific and well defined pattern over the whole heart before every normal heartbeat, resulting in potential differences at the surface of the body that can be easily measured with specific surface electrodes producing a signal known as Electrocardiogram (ECG) [9, 10]. The ECG signal has an extreme importance due to is potential as a diagnose and research tool.
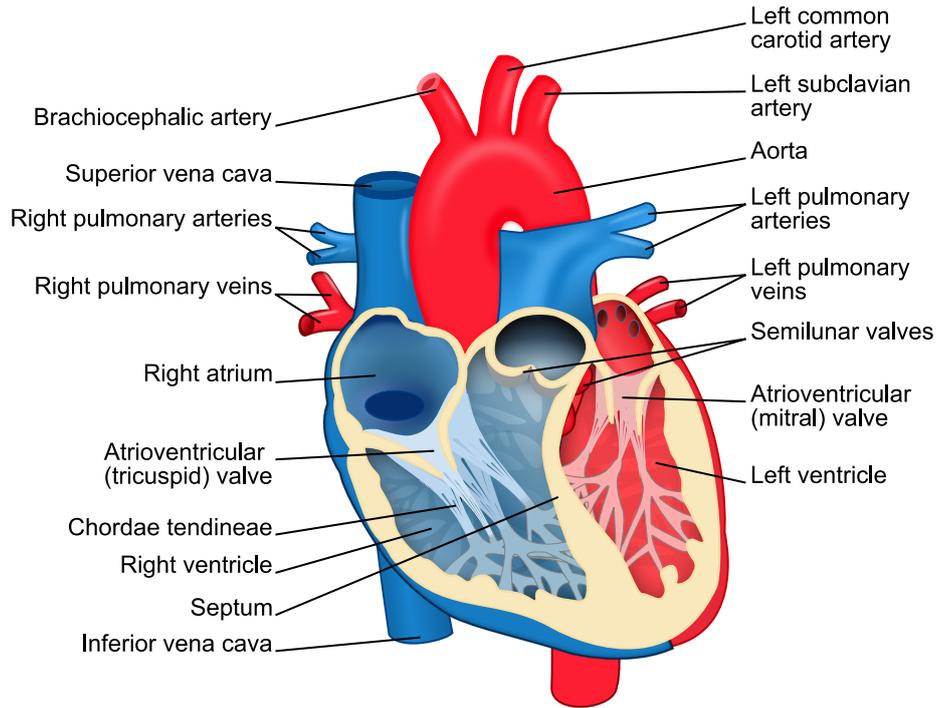
Figure 2.1: Heart diagram. Taken from [1].

2.1.1 Electrophysiology of the heart

To better realize the electrical behavior of the heart, it is necessary to analyze the behavior of a single heart muscle cell (myocyte) (see Figure 2.2), then understand the organization of the electrical structure of the heart and finally, understand how the electrical waves travel through that structure.

The cardiac muscle that forms the middle layer of the heart walls, more precisely the *myocardium*[1], is a specific kind of muscle that is composed of heart muscle cells called *myocites*. The process of electric depolarization of the myocytes occurs by the inflow of sodium ions across the cell membrane while the repolarization is achieved by the outflow of potassium ions across the cell membrane, producing an action potential similar to that of nerve cells (around 100 mV). However, the duration of the cardiac impulse is higher than the one verified in the nerve cell or even in the skeletal muscle.

One of the most important differences between the tissue from skeletal and cardiac muscle tissues is that, despite the presence of *striations* in both, the second type of muscle can transmit the electric activation from one cell to any of the adjacent ones

---

[1]The thick, contractile middle layer of uniquely constructed and arranged muscle cells (cardiac muscle) that form the bulk of the heart wall [11].
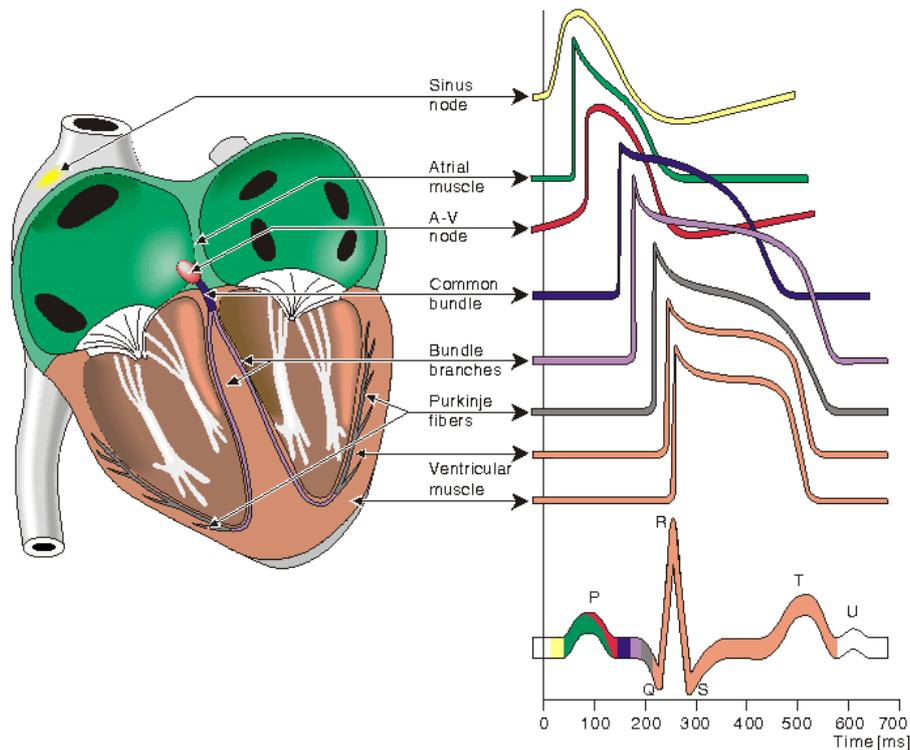
Figure 2.2: Electrophysiology of the heart.The different waveforms for each of the specialized cells found in the heart are shown. The latency shown approximates that normally found in the healthy heart. Taken from [2].

thanks to the presence of gap-junctions[2], which means that the electrical waves can be spread in any direction [2, 10].

To ensure the heart electrical activity the myocardium has a series of localized nodes with specific electrical roles, responsible for the electrical discharges that happen periodically within the heart, which induces the muscular activity of the heart and consequently the blood pumping throughout the body.

In normal conditions, the heart, is first stimulated by the *SA node* [12], that is localized in the right atrium at the superior vena cava (see Figure 2.2) and is the primary *pacemaker*[3] of the heart. Given the self-excitatory properties of the nodal-cells, this node has the responsibility to activate the muscular cells in the right atrium and to propagate the activation to the rest of the atria, initiating the heartbeat. It has an intrinsic frequency of 100 to 120 beats per minute (bpm). However, the resulting frequency is normally lower, on the order of 70 bpm, due to the complex nature of the processes occurring since the initial stimulation until the complete depolarization of the

---

[2]Low-resistance pathways that interconnect cardiac muscles.

[3]A myocardial cell displaying automaticity.

atria. The activation is then transmitted to the ventricles through the *Atrioventricular (AV) node*, since the electrical impulse cannot cross through the non-conducting fibrous barrier that separates the atria from the ventricles.

The AV node is located at the boundary between the atria and the ventricles (see Figure 2.2), and provides the only path for the electrical waves to reach the ventricles, as noted above. It works like a secondary pacemaker that, in case of fail in the electrical reception, will set the beat at a lower frequency (50 bpm). When the electrical impulses reach the AV node, coming from the SA node, the beat will be set normally, since the SA node has an higher frequency which inhibits the one set by the AV node. Moreover the AV node works as a safety system that momentarily delays the propagation of the electrical potential, avoiding the consequences of rapid atrial potentials arriving to the ventricles.

After the electrical potential has crossed the mentioned barrier, it enters the *bundle of His*, which is a specialized conducting system that has a bifurcation into two *bundles branches* (right and left) at the septum. Latter, each bundle ramifies into *Purkinje fibers*. This structure provides the propagation of the electrical impulses from the AV node to the ventricles. As this propagation happens, the ventricular depolarization takes place at a very high speed. *Purkinje fibers* work as a third *pacemaker* (15-30 bpm) avoiding any AV node fail.

A refractory period, during approximately 200 ms, where no electric potential can flow through the myocardium, follows the depolarization of the ventricles. Then, a repolarization occurs restoring the *myocardium*'s resting potential and leaving the heart ready to undergo a new cycle.

As it was described above, the intrinsic frequency of the SA node is the highest among the heart *pacemakers*. This fact makes the SA node the main *pacemaker* of the heart which means that it sets the working frequency of the whole heart [2, 9, 13].

2.1.2   The ECG

An ECG is the result of a graphical recording of the potential differences that are generated at the surface of the thorax during the electrical activity of the heart, using specific surface electrodes and acquisition hardware. Willem Einthoven received the Nobel Prize in Physiology or Medicine in 1924 for his work on "the discovery of the
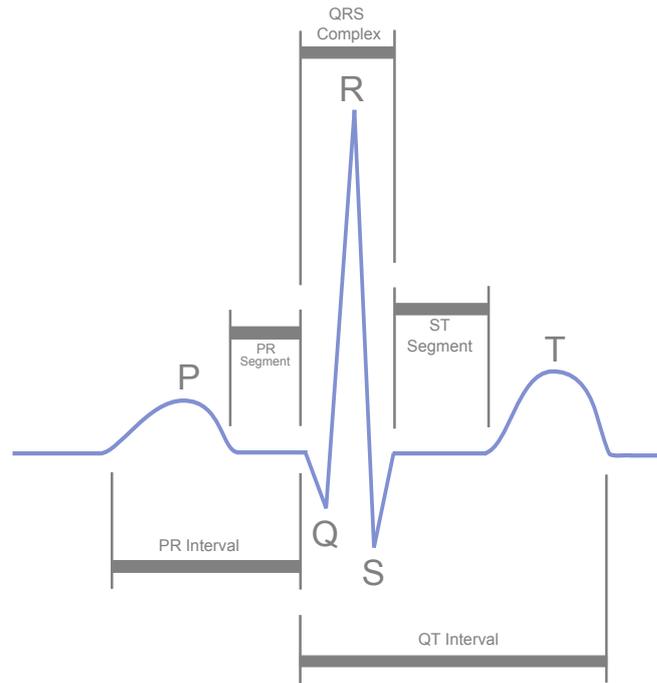
Figure 2.3: Normal features of the ECG. Adapted from [3].

mechanism of the ECG". Einthoven assigned the different patterns of the ECG and described the manifestations of a significant number of disorders on the ECG waveform [14].

As seen in 2.1.1 the electrical propagation in the heart follows a specific pattern throughout the electrical pathway. This pattern determines the shape of the ECG waveform in normal and abnormal situations. In normal situations, the ECG has the shape present in Figure 2.3. This schematic representation shows the initial P-wave, the main QRS complex and the T-wave. Each of these waves are caused by specific and sequential events that happen along the electrical pathway. The P-wave corresponds to the depolarization of the atria that happens before atrial contraction. This wave has a low amplitude due to the few quantity of muscle present in the atria. The QRS complex, which is the highest portion of the ECG waveform and happens simultaneously to the atrial repolarization (not observable in the ECG), reflects the different moments of ventricular depolarization. Finally, the T-wave represents the ventricular repolarization. The period during which ventricular contraction occurs is known as *systole*, while the period between ventricular contractions is known as *diastole*.

The description given above refers to the most common shape of the ECG. However, that shape can vary among healthy patients and between healthy and non-healthy

patients [2, 9].

The simplest mathematical model that describe the electrical activity of the heart is known as the "single dipole" model. This model considers the propagation of an action potential between adjacent cardiac cells, as the elementary source of the surface ECG. The intracellular current propagation at the interface of depolarizing and resting tissue forms the the current dipole. The propagation, in the opposite direction, of extracellular current promotes the charge conservation and forms the dipole field. The electrical activity of the heart boils down to a single equivalent dipole whose magnitude and direction correspond to the summation of all the individual dipoles (the time-dependent heart vector M(t)). Since the surface distribution of potentials varies with the body properties, the dipole model assumes that the body is a linear, isotropic, homogeneous and spherical conductor [2].

Understanding of the dipole model is important in order to know the heart vector pattern and to know how to deal with it to accurately acquire the ECG signal.

2.1.3   Abnormalities in the ECG pattern

One of the greatest achievements that ECG has made possible, was the possibility to diagnose cardiac problems through the analysis of an ECG record. The identification of abnormal situations in ECG waveform pattern is of extreme importance to clinicians.

If the SA node fails to initiate the activation of the heart, due to interruptions in the signal transmission along the electrical pathway, each of the other pacemakers could take care of this task. This property of the heart is almost like a plan-b, a normal compensatory response that prevents the heart activity from stoping. This phenomenon is known as *escape beats* and will lead to abnormal patterns in the ECG, depending on which alternative pacemaker is used.

Another phenomenon that will lead to *non-sinus* (not normal) pattern is known as *ectopic beats*, beats that occur earlier than expected and have a significantly different morphology. Ectopic beats, are beats that were not originated in the SA node due to, for example, drugs (e.g., caffeine) or viral infection of the myocardium. They can arise from almost every location in the heart, although the most common are known as *atrial*, *AV junctional* or *Ventricular Ectopic Beats (VEBs)*, also called Premature Ventricular Contraction (PVC)(see Figure 2.4). They and are normally characterized
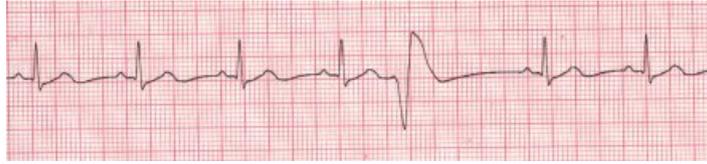
Figure 2.4: Ventricular ectopic beat. Taken from [4].

by a broad QRS complex, which happens due to a change in the system used to conduct the action potentials (myocardium instead of the high-speed *Purkinji* system). Many studies point that these events may be a consequence of poor recovery after traumatic events or may indicate the onset of fatal arrhythmias[4] [10].

The identification of ectopic beats, specially VEBs, and another abnormal ECG waveform patterns, are extremely important to detect repeating patterns with pathologic origin, such as the *Ventricular Tachycardia (VT)* and *fibrillation* (atrial and ventricular), that may cause serious damages in the heart and be fatal, by setting depolarization rates incompatible with the pumping rate of the heart or causing *circulatory arrest*[5] [9, 10].

Other types of abnormalities that can be detected with the analysis of the ECG waveform pattern are arrhythmias associated with slow rhythms (*bradycardia*), blockages in the normal propagation of the electrical activation and *ischemia*[6].

2.2 Autonomous nervous system and heart rate control

As previously discussed, the SA node acts as the primary pacemaker of the heart, setting, in normal conditions, the working frequency of the heart (HR). The SA node activity is regulated by the CNS, more precisely by the ANS, known as the involuntary motor system. The ANS is responsible for the regulation of internal organs (heart, digestive tract, lungs, bladder and blood vessels). Although the majority of these functions happen unconsciously, there are some involuntary functions that occur consciously, like breathing.

---

[4]Any variation from the normal (sinus) rhythm of the heart.

[5]Termination of blood flow through the cardiovascular circuit.

[6]When part of the myocardium is not receiving enough blood flow, often caused by disease of the coronary arteries. It will ultimately progress to myocardial cell death.

The ANS is divided into two sub-systems, the *sympathetic* and *parasympathetic nervous systems*. These two systems exert opposite and competing regulating tasks on most organs. The heart is not an exception, since it is innervated by both.

The sympathetic nervous system is often referred to as the "fight or flight" response, since it is activated during physically or mentally stressful situations. It is responsible for HR raising due to the increase in the SA stimulation and for increasing the strength of contractions due to an increase in the propagation velocity of the depolarization wave that travels through the heart (slower response - about 5 seconds). The parasympathetic nervous system is like the "rest and digest" mechanism, since it slows down the HR, decreases the Blood Pressure (BP), and increases the digestive system activity (faster response - less than 1 second).

Sympathetic and parasympathetic branches of the ANS interact in an opposite and highly complex way. However, this should be seen more like a complementary interaction rather than a competing interaction. This complementary modulation is known as the *sympathovagal balance*, which is achieved through the regulation of the levels of activation of the body (*vagal and sympathetic tone*).

In the specific case of the heart, the vagal regulation is mediated through release of *acetylcholine*, while the sympathetic regulation is mediated via release of *epinephrine* and *norepinephrine*. The acetylcholine promote the response of muscarinic receptors. These receptors, when activated, promote the decrease in the speed of the myocardium depolarization and consequently a decay in the HR. The epinephrine and norepinephrine, as expected, have an opposite behavior. They activate the β-adrenergic receptors, resulting in the acceleration of the myocardium depolarization and finally in an higher cardiac frequency. This dual regulation does not have a direct effect on the SA node, but change its sensitivity.

In addition to the central control, there are several different receptors in the cardiovascular and central nervous systems which are responsible for feedback mechanisms that can provide quick reflexes, such as tachycardic or bradycardic reflexes on the heart rate. One example of such mechanisms is the arterial baroreflex. It lies upon baroreceptors which are located on the walls of some large vessels and causes increases in vagal activity and decreases in sympathetic activity due a rise in the blood pressure. When the pressure increases, the vessels are stretched causing a rapid augmentation in
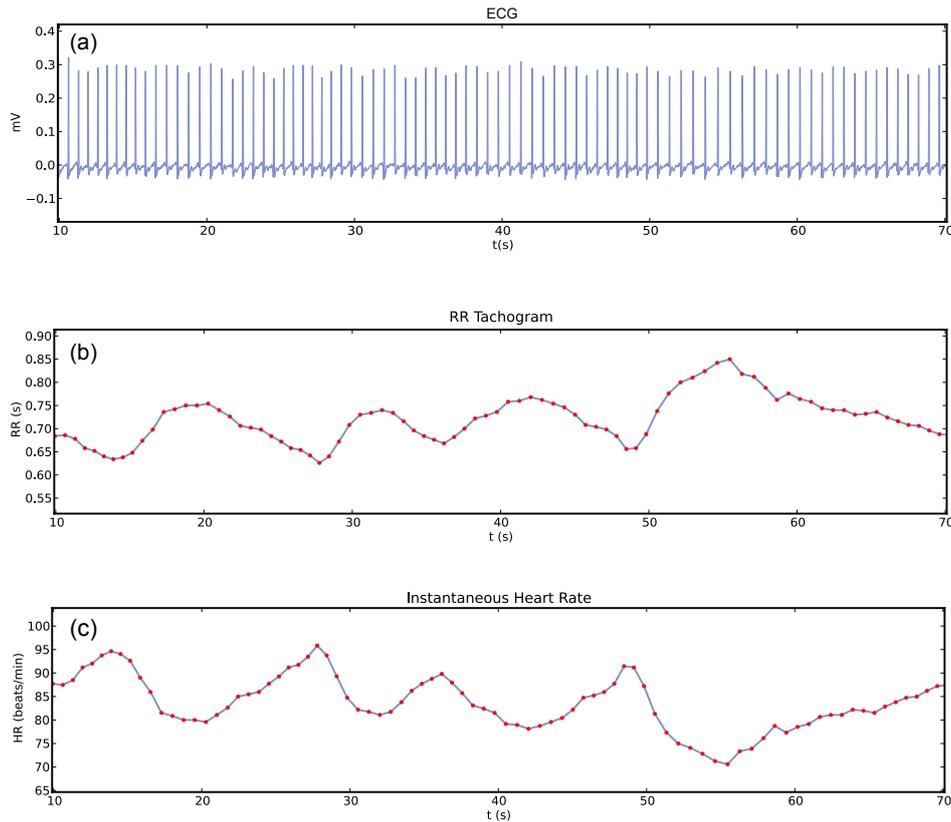
Figure 2.5: ECG segment with 60 seconds (a), the respective RR intervals (b) and the respective ₁HRs (c).

baroreceptor discharge rate leading to a bradycardic effect on the heart rate in order to lower the pressure.

It is important to note that in resting conditions, both autonomic branches are thought to have a small baseline activity with a slightly vagal predominance. Therefore oscillations in the HR are mainly dependent on vagal modulation [6, 9, 10].

2.2.1   Heart rate autonomous control and sympathovagal balance

The increase and decrease of the HR, more precisely, the Instantaneous Heart Rate (₁HR), is a consequence of the continuous modulation of the heart (SA node) by the vagal and sympathetic branches of the ANS, as previously noted (see Section 2.2). This modulation is responsible for oscillations in the interval between consecutive heartbeats as well as the oscillations between consecutive ₁HRs. In Figure 2.5, it is possible to see the oscillations between consecutive RR intervals and oscillations between consecutive ₁HRs of a typical ECG segment.

Many terms were used in the past, but "HRV" has become the term currently widely accepted to describe such phenomenon.

Since Heart Rate Variability (HRV) describes the variations in the interval between consecutive heart beats, it has been pointed out, along the last three decades, as a powerful marker of the activity of the ANS, namely the sympathovagal balance [6, 9].

Chapter 3

Heart Rate Variability Analysis

Heart Rate Variability (HRV) is a well studied phenomenon that describes the temporal variation in the intervals between consecutive heartbeats in sinus rhythm. The analysis of this phenomenon and its clinical utility is the main focus of this work.

During the last three decades several studies have been under taken in order to study the validity of HRV analysis as a quantitative and non-invasive solution to help clinicians to better understand the relationship between the ANS and cardiovascular mortality [6]. Since the rhythm of the heart is continuously modulated by the ANS through the SA node, the variability in the heartbeats periods is a consequence of such modulation and reflects the sympathovagal balance. Therefore, the metrics used to study HRV will reflect the modulation that is made by the two branches of the ANS (Sympathetic and Vagal branches) on the SA node, reflecting the sympathovagal balance [10].

The HRV analysis is based in the ECG recording, from which the HRV time series can be obtained. In order to accomplish such task it is fundamental to: firstly, to record the ECG with a high sampling frequency (500-1000 Hz) to ensure an accuracy of 1-2 ms; secondly, to determine the instants in time when the heartbeats occur; and finally, to use these time instants to calculate the heartbeats periods. Therefore, it is necessary to detect in the ECG the SA node pacing times. This is not a simple task since the portion of the ECG that is nearest from that time instants is the P-wave, which is quiet difficult to detect in several situations, due to its low magnitude potentials. However, the R peak, that is part of the QRS complex, is a valid and easy to detect alternative to extrapolate the heartbeats time instants and, consequently, the heartbeats periods.
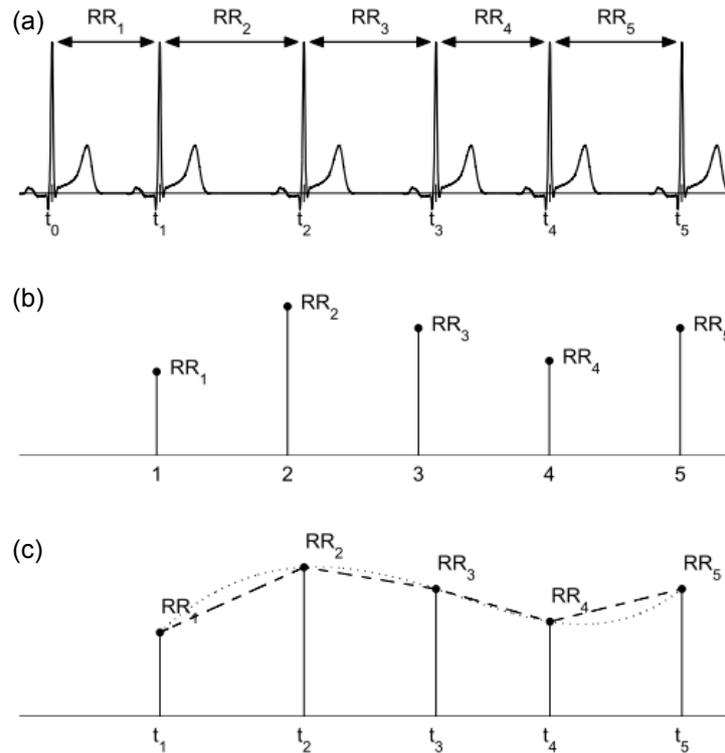
Figure 3.1: Derivation of an HRV signal from ECG: derived RR intervals (a), the interval tachogram (b) and interpolated RR interval series (c). Adapted from [5].

Therefore, the heartbeat period is defined as the time difference between consecutive R peaks ($RR_n = t_n - t_{n-1}$) and is also known as inter-beat interval, or as RR interval. It is common to see the expression NN intervals instead of RR intervals in the literature. It means normal-to-normal intervals and is used to refer the intervals between QRS complexes resulting only from SA node depolarization, excluding the intervals resulting from other pacemakers. The term RR interval will be adopted in this work.

To proceed with the R peak detection, it is necessary to use a QRS detector, normally by preprocessing the ECG followed by a decision criteria (to be discussed in Chapter 5).

After the R peak time instants are identified, it is possible to derive the HRV time series. The whole process is summarized in Figure 3.1 and results in the RR interval tachogram where all the RR intervals are registered (see Figure 3.1(b)). Such registry is the basis of the HRV analysis. For time domain as well as for non-linear HRV analysis it is possible to use the tachogram directly. In the case of frequency domain HRV analysis, this analysis can not be performed directly from the tachogram, since the data is not equidistantly sampled. Thus, for frequency domain analysis there is a need

for interpolation (e.g., linear or cubic spline interpolation) in order to equidistantly sample the data (see Figure 3.1(c)).

The HRV time series is very sensitive to technical and physiological artifacts. Physiological artifacts are normally due to arrhythmias and ectopic beats. Therefore, it is highly recommended to combine manual and automate methods, in order to inspect and correct such perturbations in the signals prior to performing the analysis [5,6].

In the following sections, the standard measurements used for evaluating HRV and later implemented in our GUI, will be presented and briefly explained, along with the clinical relevance of such analysis.

3.1 Historical perspective

The revelation of HRV as an interesting phenomenon with clinical relevance and potential happened in 1965, during Hon and Lee's research. This research showed alterations in the RR intervals duration, even before any alteration has been detected in the HR. However, the phenomenon itself has been discovered in the early 1600s [9].

Since the first studies performed by Hon and Lee and due to the extraordinary development that happened during the last decades in the signal processing techniques, the analysis of HRV have been going through a considerable evolution. Ewing *et al.*, in the 1970s, detected DAN in diabetic patients with simple tests performed on the RR intervals. Still in the 1970s Wolf *et al.* showed that there was a correlation between reduced HRV and an higher risk of post-infarction mortality. Already in the 1980s, the autonomic control of HRV was showed by Akselrod *et al.* due to the power spectral studies and the HRV has been confirmed has a "strong and independent predictor following an acute **MI!** (**MI!**)" [6,9].

In 1996, an huge step towards the standardization of nomenclature and methods was done by the Task Force of The European Society of Cardiology and The North American Society of Pacing and Electrophysiology. This task force was responsible for writing a guideline with the standard metrics, physiological interpretation and clinical applicability of HRV [6,8].
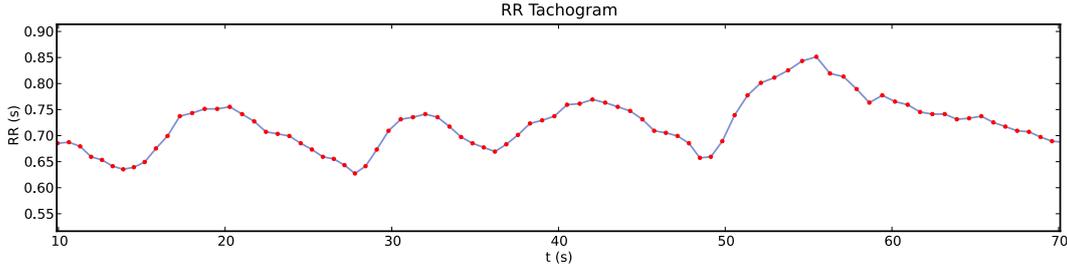
Figure 3.2: RR tachogram example.

3.2   Standards of measurement

In this section, the standard methods normally used in HRV analysis will be described. All the methods are derived from the HRV time series (RR tachogram) (see Figure 3.2) and are divided into three different categories (time domain, frequency domain and non-linear methods). Both the time and frequency domain methods adopted in this work follow the standards suggested by the Task Force of The European Society of Cardiology and The North American Society of Pacing and Electrophysiology [6].

3.2.1   Time domain methods

Since the time domain methods are applied directly to the RR interval series they are the simplest ones to compute. These methods are further divided into statistical and geometrical methods. The geometrical measures are derived from the RR interval histogram and are relatively insensitive to the analytical quality of the RR series. However, while the available time domain methods can be applied to short and long-term recordings, the current geometric methods are inappropriate to evaluate short-term recordings.

Statistical methods

- The mean value of RR intervals (ms) and Mean Heart Rate (bpm), defined by Equations 3.1 and 3.2, respectively.

$$\overline{RR} = \frac{1}{N} \sum_{j=1}^{N} RR_j \tag{3.1}$$

$$\overline{HR} = \frac{1}{\overline{RR}} \tag{3.2}$$

- SDNN (ms) - Standard deviation of the RR intervals, which reflects the overall (both short-term and long-term) variation within the RR interval series. SDNN is defined in Equation 3.3, where RR_j denotes the value of $j'th$ RR interval and N the total number of successive intervals.

$$SDNN = \sqrt{\frac{1}{N-1}\sum_{j=1}^{N}(RR_j - \overline{RR})^2} \tag{3.3}$$

- SDANN (ms) - Standard deviation of the averages of RR intervals in all 5 min segments of the entire recording, which is an estimate of the changes in HR due to cycles longer than 5 min. SDANN is given by Equation 3.4, where $\overline{RR_5}$ is the average of all 5 min RR intervals averages, RR_{5_j} denotes the value of $j'th$ 5 min RR interval average and N is the total number of successive 5 min RR intervals.

$$SDANN = \sqrt{\frac{1}{N-1}\sum_{j=1}^{N}(RR_{5_j} - \overline{RR_5})^2} \tag{3.4}$$

- SDNN index (ms) - Mean of the standard deviations of all RR intervals for all 5 min segments of the entire recording (24h), which measures the variability due to cycles shorter than 5 min. This statistical parameter is given by Equation 3.5, where $SDNN_{5_j}$ is the standard deviation of $j'th$ 5 min RR interval and N the total number of successive 5 min RR intervals.

$$SDNN_{index} = \frac{1}{N}\sum_{j=1}^{N}SDNN_{5_j} \tag{3.5}$$

- SDSD (ms) - Standard deviation of successive RR interval differences. It is defined in Equation 3.6, where $\Delta RR_j = RR_j - RR_{j+1}$, $E\{\Delta RR_j^2\} = \overline{\Delta RR^2}$ and $E\{\Delta RR_j\} = \overline{\Delta RR}$.

$$SDSD = \sqrt{E\{\Delta RR_j^2\} - E\{\Delta RR_j\}^2} \tag{3.6}$$

- RMSSD (ms) - Root mean square of successive differences (square root of the mean squared differences of successive RR intervals). In stationary RR series $E\{\Delta RR_j\} = E\{RR_{j+1}\} - E\{RR_j\} = 0$ and SDSD equals RMSSD. RMSSD is

given by Equation 3.7.

$$RMSSD = \sqrt{\frac{1}{N-1} \sum_{j=1}^{N-1} (RR_{j+1} - RR_j)^2} \qquad (3.7)$$

- NN50 (count) and pNN50 (%) - The number of interval differences of successive RR intervals greater than 50 ms and the corresponding percentage (Equation 3.8). Sometimes, a more restrictive measure, regarding differences under 20 ms, is calculated (i.e., NN20 and pNN20).

$$pNN50 = \frac{NN50}{N-1} \times 100\% \qquad (3.8)$$

Geometrical methods

- HRV triangular index - Integral of the density distribution divided by the maximum of the density distribution, Equation 3.9. A schematically representation of the sample density distribution of a series of RR intervals (D) can be seen in Figure 3.3, where X represents the most frequent RR interval and Y the maximum of the sample density distribution ($Y = D(X)$).

$$HRV_{index} = \frac{\int D(t)dt}{Y} \qquad (3.9)$$

In a discrete scale, this measure can be approximated by Equation 3.10. These approximation is dependent on the bin with of the histogram. A bin with of 1/128 seconds is recommended [9].

$$HRV_{index} = (\text{total number of all NN intervals})/Y \qquad (3.10)$$

- TINN (ms) - Triangular interpolation of NN interval histogram which corresponds to the baseline width of the density distribution measured through triangular interpolation. In order to compute TINN, it is necessary to select the values N and M (see Figure 3.3) and a multilinear function q such that $q(t) = 0$ for $t \leq N$ and $t \geq M$ and $q(X) = Y$, and such that the integral present in Equation 3.11
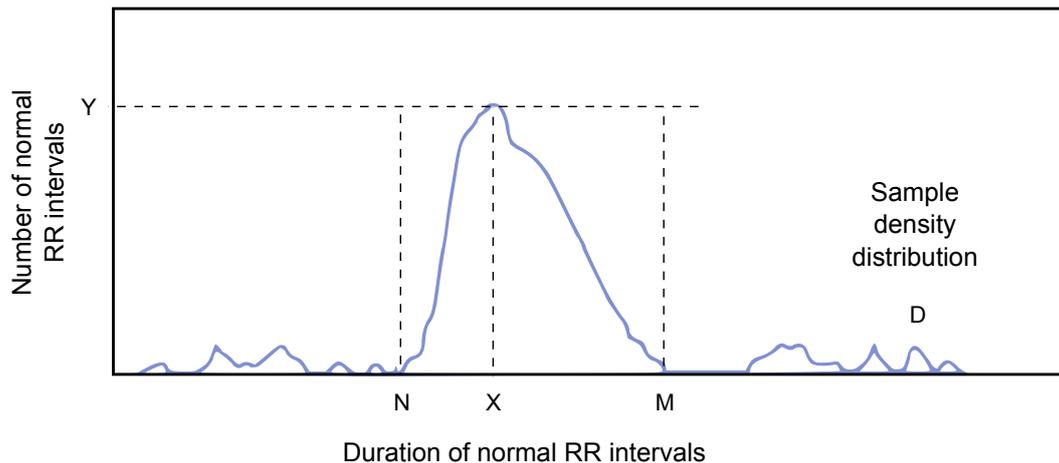
Figure 3.3: Schematic representation of the sample density distribution of a series RR intervals. Adapted from [6].

is the minimum among all selections of all values N and M. Than the TINN measure, expressed in ms, is given by Equation 3.12.

$$\int_0^{+\infty} (D(t) - q(t))^2 dt \tag{3.11}$$

$$TINN = M - N \tag{3.12}$$

3.2.2 Frequency domain methods

The variability between RR intervals occurs on a wide number of time scales. As a consequence, the analysis of tachogram's spectral components has an enormous potential for understanding the factors that contribute to the different components. The most common power spectral estimation technique used in HRV analysis is the Power Spectral Density (PSD) analysis (see Figure. 3.4).

PSD estimation provides the basic information of how the power of the signal (i.e., its variance) distributes as a function of frequency. This estimation can be made with two different type of methods: non-parametric and parametric. The non-parametric method is computationally simpler and the results obtained are very similar to the parametric results [6, 9, 10]. For that reason, this type of methodology was adopted here.

Fast Fourier Transform (FFT) computation, based on Welch's periodogram [15], is the basis of the non-parametric PSD analysis. The Welch's method estimates the
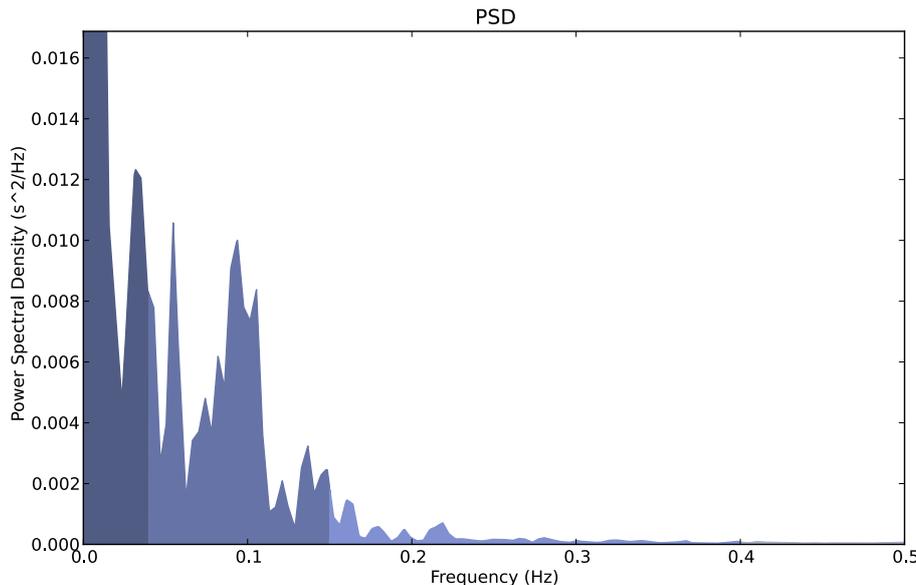
Figure 3.4: Power spectral density spectrum example.

power of a signal vs. frequency and is an improvement of the standard periodogram method and Bartlett's method. It is based on the Bartlett's method but with two main differences:

- the original data segment is split up into L data segments of length M, overlapping by D points (if D = M/2, the overlapping is said to be 50%, and if D = 0, the overlapping is said to be 0%, that is what happens in the Bartlett's method);

- the overlapping segments are then windowed with a specific window (e.g., a Hanning window).

After the overlapping and windowing steps, the periodogram is calculated using the discrete FFT, and then the squared magnitude of the result is computed. Each of the individual periodograms is then time-averaged, reducing the variance of the individual power measurements [15].

Since PSD estimation assumes that data is equidistantly sampled, the RR interval series has to be previously interpolated. In order to obtain the best results, it is suggested to adopt a cubic interpolation with a 4 Hz interpolation frequency [5, 9].

The main spectral components in a spectrum calculated from short-term recordings, differ from the spectral components in a spectrum calculated from long-term recordings. In the first case the spectrum has three main spectral components: Very Low Frequency

(VLF), Low Frequency (LF) and High Frequency (HF) components that are comprised, respectively, in the ranges 0-0.04 Hz, 0.04-0.15 Hz and 0.15-0.4 Hz. In the second case, a new component is introduced, the Ultra Low Frequency (ULF) component, comprised in the range of 0-0.003 Hz. The VLF component becomes comprised between 0.003 and 0.04 Hz. The other frequency components, (LF and HF) remain unchanged.

Table 3.1: Summary of the HRV frequency domain parameters. Adapted from [5]

Measure	Units	Description
Peak frequency	Hz	VLF, LF and HF band peak frequencies
Absolute power	ms^2	Absolute powers of VLF, LF and HF bands
Relative power	%	Relative powers of VLF, LF and HF bands:
		VLF [%] = VLF $[ms^2]$/total power $[ms^2]$ $\times$ 100%
		LF [%] = LF $[ms^2$/total power $[ms^2]$ $\times$ 100%
		HF [%] = HF $[ms^2]$/total power $[ms^2]$ $\times$ 100%
Normalized power	n.u.	Powers of LF and HF bands in normalized units:
		LF [n.u.] = LF $[ms^2]$/(total power $[ms^2]$ - VLF$[ms^2]$)
		HF [n.u.] = HF $[ms^2]$/(total power $[ms^2]$ - VLF$[ms^2]$)
LF/HF		Ratio between LF and HF band powers (LF$[ms^2]$/HF$[ms^2]$)

In order to obtain the absolute power values for each frequency component a *Simpson's integration* is performed between the component limits. Although absolute values are normally used, the LF and HF components may also be measured in normalized units which reflects the relative value of each power component in proportion to the total power without the VLF component and highlights the controlled and balanced behavior of the ANS.

Table 3.1 summarizes the parameters extracted from the PSD analysis. The analysis includes: absolute and relative powers of each frequency component, normalized powers of LF and HF components, the LF/HF power ratio and the peak frequencies for each component.

3.2.3 Nonlinear methods

Considering that the heart has a complex control system and that HR fluctuations have an irregular behavior, it is easily understandable the need to implement methods that could describe such complexity and irregularity. In this context, nonlinear methods, based on chaos theory and fractal analysis, have been applied in order to better understand the nonlinear phenomena underlying HRV [16].
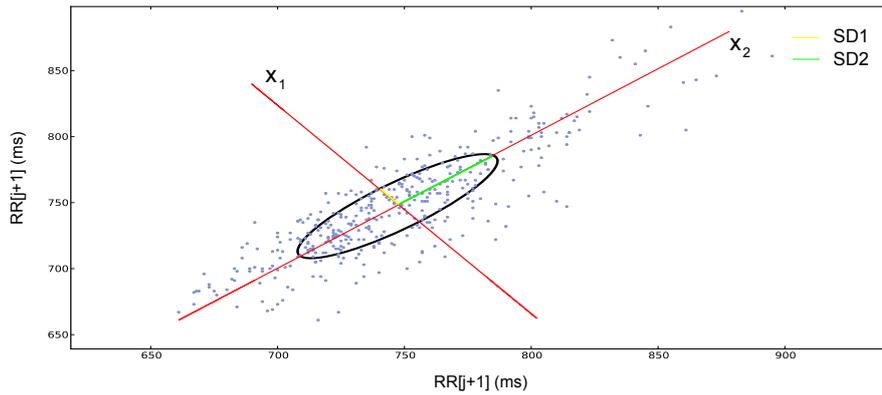
Figure 3.5: Poincaré plot analysis with the ellipse fitting procedure. SD1 and SD2 are the standard deviations in the directions x_1 and x_2, where x_2 is the line-of-identity for which $RR_j = RR_{j+1}$. Adapted from [5].

Poincaré plot and ellipse fitting procedure

One of the nonlinear techniques that is getting a significantly popularity in the scientific community is the *Poincaré plot*, due to its simple visual interpretation and its proven clinical applicability [17].

Poincaré plot is a graphical projection of RR_{j+1} as a function of RR_j. It reflects the graphical correlation between consecutive RR intervals. A common strategy to statistically characterize the shape of the plot is to use an ellipse fitting technique, where an ellipse is adjusted to the plot and oriented according to the line-of-identity ($RR_j = RR_{j+1}$). The axis of the ellipse fitted to the plot are related to the axis of the Poincaré plot by a rotation of $\theta = \pi/4$ rad described by Matrix Equation 3.13 (see Figure 3.5).

$$\begin{bmatrix} x_1 \\ x_2 \end{bmatrix} = \begin{bmatrix} \cos\theta & -\sin\theta \\ \sin\theta & \cos\theta \end{bmatrix} \begin{bmatrix} RR_j \\ RR_{j+1} \end{bmatrix} \tag{3.13}$$

The dispersion of points perpendicular to the line-of-identity mirrors the level of short-term HRV (SD1 - standard deviation of the points perpendicular to the line-of-identity) which is mainly caused by Respiratory Sinus Arrhythmia (RSA)[1]. On the other hand, the dispersion along the line-of-identity is thought to reflect the level of long-term HRV (SD2 - standard deviation along the line-of-identity). It can be proved that short and long-term dispersion are related to the time-domain measures SDSD

---

[1] Phenomenon of ₁HR acceleration on inspiration, and its deceleration on expiration.

and SDNN according to Equations 3.14 and 3.15, respectively. Assuming stationarity
in the RR series, SDSD equals RMSSD and RMSSD can be used instead [5, 17].

$$SD1^2 = \frac{1}{2}SDSD^2 \tag{3.14}$$

$$SD2^2 = 2SDNN^2 - \frac{1}{2}SDSD^2 \tag{3.15}$$

Equations 3.14 and 3.15 allow for the extraction of extra HRV indexes (SD1 and
SD2), that describe quantitatively the short and long-term fluctuations. These two
indexes correspond to the minor and major axis of the ellipse, as can be seen in Figure
3.5. The ratio between these two indexes (i.e. SD1/SD2 ratio) is usually computed.

Additionally to the first order poincaré plot (RR_j, RR_{j+1}), described above, three
dimensional second order poincaré plots $(RR_j, RR_{j+1}, RR_{j+2})$ and poincaré plots with
a bigger lag (e.g., (RR_j, RR_{j+2})) can also be implemented [5, 17].

3.3   Clinical and physiological importance of HRV analysis

Due to the correlation between HRV and the autonomic heart modulation, the potential
of HRV analysis as a tool for clinical use is obvious. Spectral analysis applied to HRV
allowed a better understanding of the SA node autonomic modulation. Such analysis
revealed clearly that the vagal activity is the major contributor to the HF component.
It also revealed that the RSA has an important contribution to the HF band. In
the LF component the results were not so conclusive and are currently a matter of
discussion: there are some researchers that defend the LF component as a marker of the
sympathetic activity (specially when it is expressed in normalized units (n.u.)), whereas
others defend that it is a marker with both sympathetic and vagal contributions. Some
researchers also defend that the LF/HF ratio reflects the sympathovagal balance or the
sympathetic modulations. In the lower frequency components of HRV (VLF and ULF
components) further research is needed because the physiological correlations are still
unknown [6, 9, 18].

Several studies reporting changes in HRV associated with specific pathologies have

been conducted. The reported pathologies that were associated with such changes are:

- **MI!** - Depressed HRV is a strong predictor of mortality and of arrhythmic complications in patients who had an acute **MI!**. After acute **MI!** the decrease in HRV may mirror a reduction in the vagal activity at the SA node level which could lead to electrical instability. These facts are shown mainly by the spectral analysis of HRV which revealed a reduction in total and in the individual power of spectral components. The HRV predictive value is independent of other factors established for post-infarction risk stratification [6, 8, 9, 19, 20].

- Diabetic Autonomic Neuropathy - It was shown that a reduction in time domain parameters of HRV comprises a prognostic value and precedes the clinical expression of DAN in patients with *diabetes mellitus*. These patients also showed a reduction of the absolute power of LF and HF components during controlled conditions [6, 9, 19].

- Congestive cardiac failure - Nolan *et al.* [20] demonstrated that a reduction in HRV (SDNN) was the most powerful predictor of all cause of mortality, among all parameters, in patients with such disease (left ventricular systolic diameter, serum sodium and cardiothoracic ratio).

- Cardiac transplantation - Patients whose heart has been recently transplanted were reported to show a very depressed HRV without any evident spectral components. These facts are considered to reflect the absence of re-enervation, which may occur only 1 to 2 years after the cardiac transplantation [6, 9].

- Myocardial disfunction - A reduced HRV in patients with cardiac disfunction has been repeatedly reported. The depression was observed in both time and spectral domain measures. If in the first case the reduction observed seems to correlate positively with the severity of the disease, in the second case the correlation does not appear so simple. In particular, in the majority of the patients in a very advanced state of the disease and with a drastic reduction in HRV, a LF component could not be detected despite clinical signs of sympathetic activation. Therefore, in such situations, the SA node seems to diminish its responsiveness to neural stimulus [6, 9, 19].

- Tetraplegia - Patients with such clinical condition are an extremely important clinical model since they lose the modulatory control of the spinal sympathetic neurons and the baroreflex supraspinal inhibitory inputs but preserve intact the efferent vagal and sympathetic neural pathways to the SA node. This is an unique scenario to evaluate the contribution of supraspinal mechanisms in determining the sympathetic activity responsible for low frequency phenomena [6, 9, 19].

- There are several other situations that were shown to induce significant modifications in the HRV. A few examples are: β-adrenergic blockers, antiarrhythmic drugs, muscarinic receptors blockers, thrombolysis and exercise [6, 9].

Despite all the studies performed to evaluate the correlation between the HRV and a wide range of diseases and clinical conditions, the only two which obtained a generalized consensus in the research community were the association between HRV and the risk after acute **MI!** and between HRV and DAN [5, 6].

Chapter 4

Photoplethysmography as an alternative to ECG for HRV analysis

In the previous chapter we have seen that the derivation of RR interval time series is accomplished, firstly, by detecting the QRS complexes times in an ECG signal and, secondly, by computing the intervals between complexes. Although the ECG signals are a precise and reliable source of RR time series, there are some inconveniences associated with ECG recording and ECG's QRS detection. The first problem relies on the large dimensions and complicated setups of the majority of available commercial equipments developed to record ECG signals. The second problem is related with the noise and signal artifacts that often interfere in the ECG pattern leading to problems in QRS detection.

As to the first problem the acquisition system used in this project to acquire the signals (*bioPLUX reasearch* [21]) provides a good solution, thanks to its reduced dimensions and simplicity of use. Regarding the second problem, it has not been completely overcome, so far, as in same recordings the signals are affected by noise and artifacts causing bad QRS detections and the need for manual correction by the user. This scenario was analyzed by many researchers and some approaches were suggested, like the use of Arterial Blood Pulse (ABP) and Photoplethysmography (PPG) (also known as Blood Volume Pulse (BVP)) signals as an alternative to the use of ECG [22–24]. Since ABP is an invasive technique, its use for HRV analysis was excluded. PPG, as
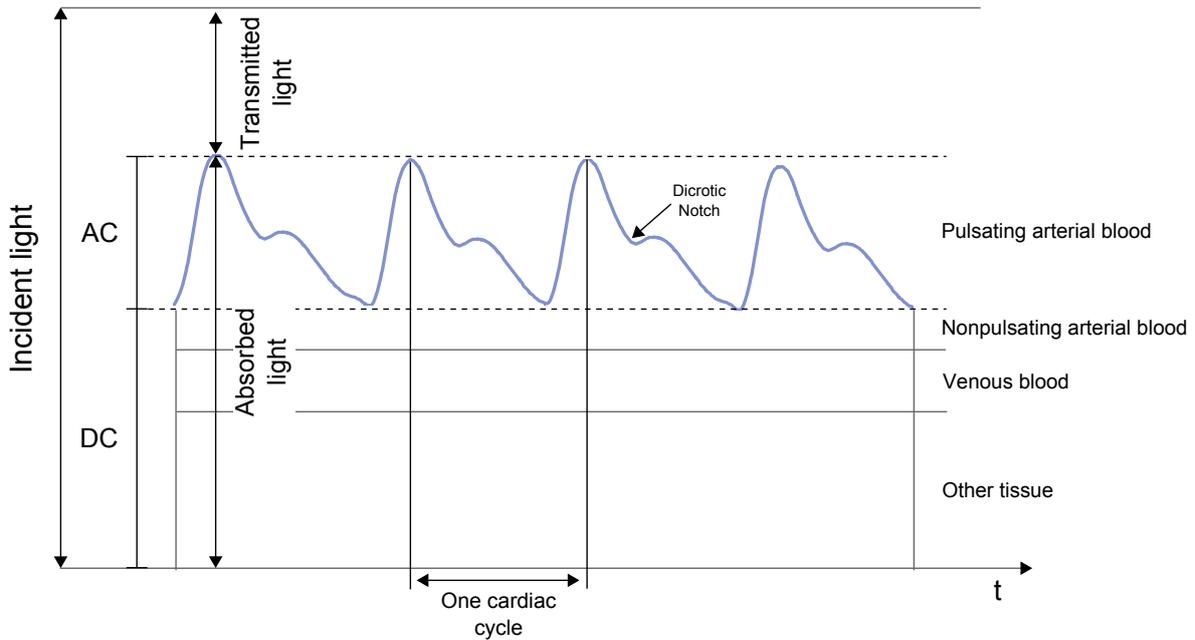
Figure 4.1: Schematic illustration of a photoplethysmogram. The signal is inverted compared to the signal from the sensor and correlates positively with blood volume. Adapted from [7]

a noninvasive method that reflects the blood changes that happen during each cardiac cycle, has a much higher potential than ABP and was studied as an alternative by a few authors [22, 23]. After a careful review of such studies we decided to explore and apply PPG as an alternative and complementary solution to ECG in our HRV analysis tool.

In the following sections a brief explanation of the PPG technique is given, as well as a short description of its potential for HRV analysis.

4.1   Photoplethysmography

PPG is an optical measurement technique that is normally used to measure the changes that occur in blood volume in a specific part of the body (e.g., fingertip and earlobe) during each cardiac cycle. This technique relies on the optical properties of the tissues, that, when illuminated by light with a specific wavelength (red or infrared) absorb, transmit and reflect that light differently, depending on the volume of blood present in the vessels. The PPG technique is also used to estimate the level of blood oxygenation, using two pulsatile LEDs and the hemoglobin absorption properties, which differ for the red and infrared light [25, 26].
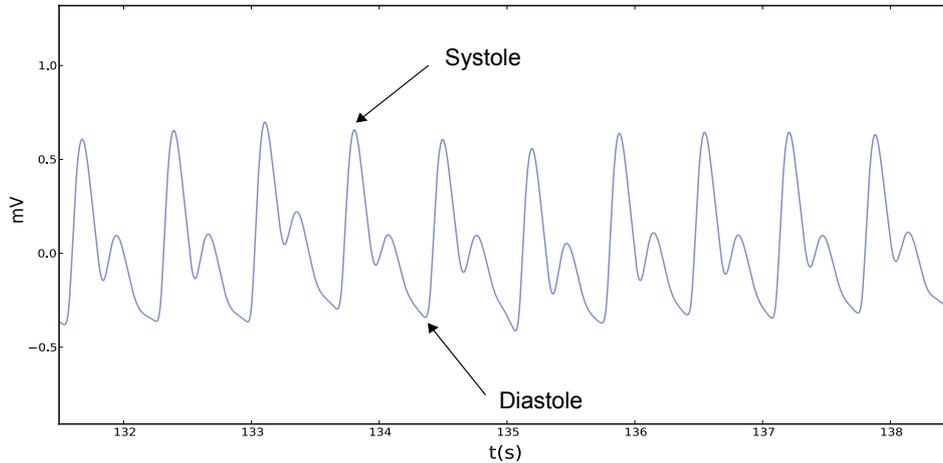
Figure 4.2: Example of a real PPG signal.

As it was described in Section 2.1.2 the cardiac cycle is known to have two main periods, systole and diastole. Systole corresponds to the period where the heart contracts and expels the arterial blood to the arteries, and diastole to the period where the heart is relaxed and receives venous blood from the veins. Since the amount of light that is detected by a PPG sensor is proportional to the volume of blood arriving from the heart in each moment, it is easy to understand that these periods will cause different levels of light detection [7].

The PPG signal has two components, a small pulsatile AC component and a large non-pulsatile DC component. The first one is due to the pulsatile blood while the second one is due to absorbance that happens in the tissues, bones, venous blood and non-pulsatile arterial blood (see Figure 4.1). Normally, only the AC component is shown since the sensor has low-pass filters that remove the DC component [7].

Figure 4.2 illustrates the alternating component of a PPG signal. By convention, the signal is inverted relatively to the light that reaches the photodetector in order to have a positive correlation with the quantity of blood that arrives to the tissues. Therefore, the peaks correspond to systoles and the valleys to diastoles.

It is important to refer that there are two different kinds of PPG sensors. The ones that detect transmitted light and the ones that detect reflected light. In the transmission type, the light is shinned by a LED and is detected by a photodetector placed on the opposite side of the tissue. In the reflection type, the light is irradiated by a LED placed on the same side of the photodetector, that measures the light reflected by the tissues.
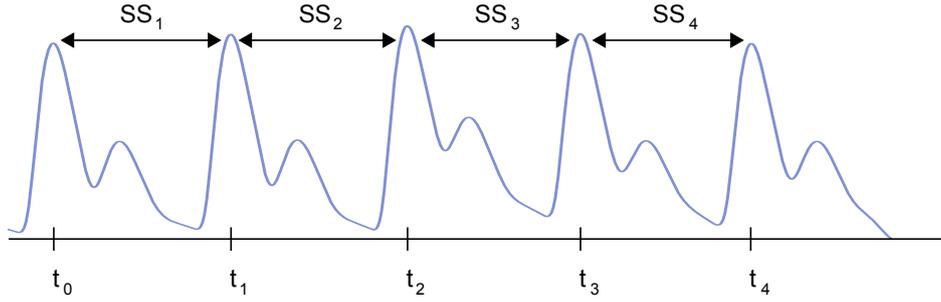
Figure 4.3: Schematic illustration of SS intervals derivation. For simplification SS intervals will be named RR intervals too.

This signal is used to measure a wide number of cardiovascular parameters and scenarios such as the already mentioned blood oxygen saturation, HR, blood pressure, cardiac output, arterial disease and Pulse Transit Time (PTT) [24].

4.2   Potential application in HRV analysis

Pulse oximeters, which allow for oxygen saturation estimation, HR monitoring and PPG signal visualization, are a widely available and often used noninvasive tool for continuous intensive care and ambulatory patient monitoring. However, few studies have been carried out to quantitatively investigate the use of PPG as an effective and sufficiently precise alternative to measure of the dynamics underlying the $_I$HR fluctuations, because the full potential of the information provided has only been realized recently [23].

The PPG signal, as described in the previous section, reflects the oscillations in the blood volume that happen in the tissues during each cardiac cycle, indicating that this signal may reflect the HRV and, in the end, the ANS dynamics. Since the sensors used to obtain such measure are less obtrusive and more user friendly than the ECG sensors, its potential as an alternative to derive the differences between consecutive heartbeats and consequently the RR time series was investigated in a few studies [22,23]. Although in PPG such derivation has to be made between consecutive systoles and not between consecutive R peaks, in the current work we decided to use the same nomenclature to simplify the description and facilitate its understanding. Thus, the systole-to-systole intervals (i.e. SS intervals) will be renamed to RR intervals (see Figure 4.3).

Lu *et al.* and Yang *et al.* [22, 23] were responsible for two researches covering this issue. These studies showed an high correlation between HRV parameters calculated

from simultaneously acquired ECG and PPG signals. However, in a few situations, they reported that motion artifacts affected PPG signals and consequently prevented the desired HRV analysis of being carried out. With such results, they concluded that PPG could be used in rather controlled scenarios, as a legitime alternative to ECG in HRV analysis.

With such information in hand we decided to implement, in the HRV tool that was being developed, an alternative way to assess HRV based on PPG signals. In order to derive RR intervals from PPG signals, we had, first, developed an algorithm to accurately detect the systoles peaks. After that, the algorithm was implemented in our software tool and used to perform a study to confirm that the PPG signal is a valuable alternative to ECG, as referred in previous studies, and also to validate our PPG sensor for HRV analysis. The methods used as well as the results obtained for such study will be presented in Chapter 6.

Chapter 5

Development of a GUI for HRV analysis

As it was described in the previous chapters, HRV is a phenomenon with a growing potential for clinical diagnosis and medical research. The absence of adequate, free and easy to use programs that perform HRV analysis have led us to develop a new full featured and multi platform Graphical User Interface (GUI) targeted at physicians and researchers. The development of such tool is justifiable and opportune, as the few free softwares available are complicated to implement (*PhysioNet HRV* [27]) or have some limitations (*Kubios HRV* [28]).

The current chapter summarize the development of a GUI for HRV analysis (called *HRV PLUX*) and describes its main features. The program was written in *Python* since it is an open source and powerful programming language known to be able to run on multiple platforms (Windows, Linux/Unix and Mac OS X) [29]. Moreover, Python was also chosen because of the set of scientific tools available for signal processing and visualization (similar to MATLAB® [30]) as well as the tools available for GUI implementation.

In order to build the HRV analysis tool we have used three different Python scientific libraries (*NumPy*, *SciPy*, and *Matplotlib*), a cross platform GUI library for Python (*wxPython*), an interactive Python shell (*IPython*) and the *eclipse* IDE with the *pydev* plugin, that provides a good support for Python development. NumPy is an open source and extremely useful extension for Python which adds support for large, multi-dimensional arrays and matrices, and has a large set of high-level mathematical

(a) File menu   (b) HRV menu   (c) Help menu
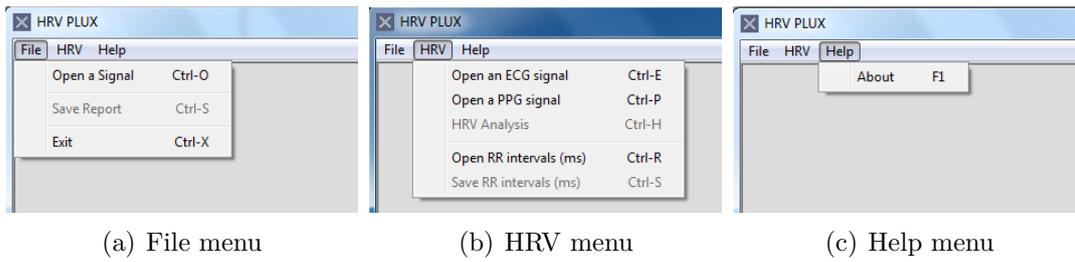
Figure 5.1: The different menus of the HRV software.

functions to operate with these arrays [31]. SciPy is also an open source library for Python with algorithms and mathematical tools, like numerical integration modules, interpolation modules, FFT modules and others useful signal processing modules, to solve scientific and engineering problems [32]. Matplotlib is an extraordinary open source Python 2D and 3D plotting library with an amazing integration in a wide variety of GUI toolkits, including wxPython [33]. WxPython is a GUI toolkit that allows to create robust and highly functional GUIs [34].

This project had three main phases. It started with an extensive research about HRV and the methods available (see Chapter 3), then the different methods were implemented in simple Python functions and classes using the scientific libraries described above and finally an interactive version of the HRV analysis tool was implemented using the wxPython library and the functions and classes previously developed.

5.1   The user interface

Python is the main resource behind this project. With the features available in this programming language, we have been able to develop a simple and interactive GUI, that integrates many signal processing functions and advanced graphical solutions, essential to implement the necessary methods for performing a complete and accurate HRV study.

In this section we will provide a general description of the main functionalities of the HRV tool that we have developed. Later in this chapter, we will explain in detail the most important features and characteristics of the tool.

The HRV software was designed to work with ECG and PPG signals acquired with a *bioPLUX research system* [21] and with RR intervals time series previously computed by this or by other software. In the first case, the R peaks of the ECG
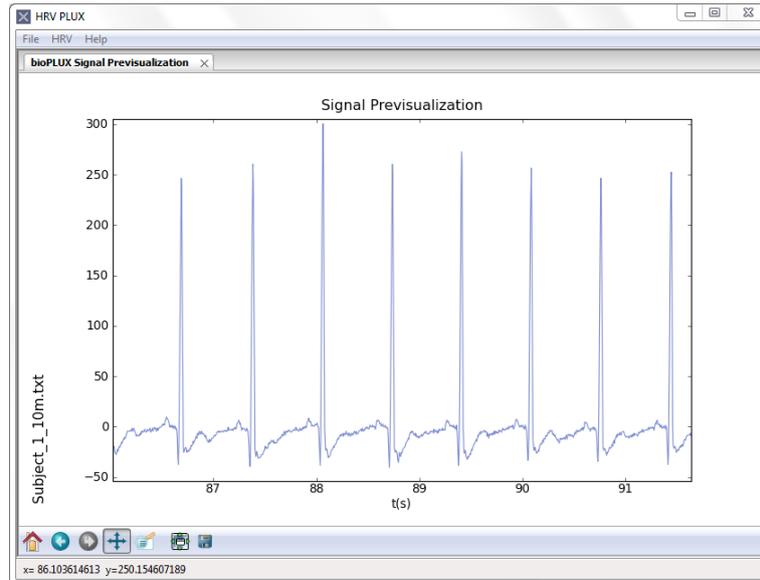
Figure 5.2: Previsualization of an ECG signal acquired with a *bioPLUX research system*.

signals and systolic peaks of the PPG signals have to be detected in order to compute the RR intervals and perform the HRV analysis. In the second case, the analysis can be performed directly.

This software has three different menus (see Figure 5.1):

- the "File" menu,

- the "HRV" menu,

- and the "Help" menu.

The most important functionalities are hidden in the first and second menus, the "File" and the "HRV" menus, respectively, while the third menu, the "Help" menu is just for informative purposes.

The "File" menu has three main options: the "Open a Signal" option that allows, once selected the *bioPLUX* channel used and the desired sampling frequency, for the previsualization of *bioPLUX* signals as shown in Figure 5.2; the "Save Report" option to save the HRV reports, that will be showed later, since it is only activated after an analysis has been performed; and finally an "Exit" option.

In the second menu the user can choose the desired source to perform the HRV analysis (i.e. ECG signals, PPG signals or RR intervals). If the first or the second option is chosen ("Open an ECG signal" or "Open a PPG signal"), the user will have
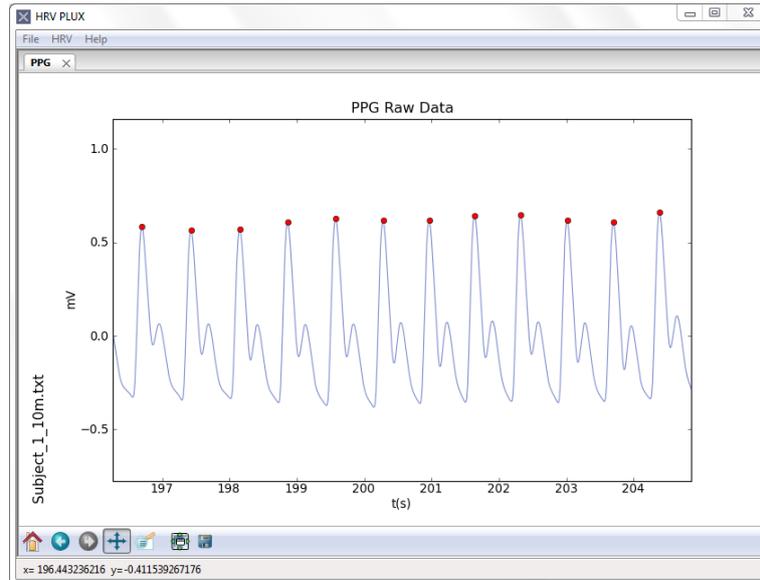
Figure 5.3: PPG signal with the systolic peaks identified with red circles.

to select the file that contains the signal and has to specify the *bioPLUX* channel used and the desired sampling frequency. After that, the signals are preprocessed (i.e. the mean is removed and the signals are digitally filtered to remove noise and baseline fluctuations), the peaks are detected and the signal with the peaks highlighted is presented in a new tab window (see Figure 5.3). Since the peak detection is often affected by noise and artifacts we have implemented a detector that highlights with different colors abnormal intervals according with their nature (i.e. skipped beats or ectopic beats) and also an interactive way to manually edit any marked peak, allowing for the correction of skipped beats (see Figures 5.4 and 5.5).

With the peaks correctly detected, the user can proceed and perform the HRV analysis, choosing the "HRV Analysis" option available in the same menu. This option will perform a wide number of computations to implement the methods previously described (Chapter 3) and generate different HRV graphics and a report with the calculated parameters. The graphics and the report will be shown in five new window tabs that can be dynamically rearranged according to the user preferences (see Figure 5.6). The report can be saved in HTML (*.html*) format for later consult, using the option "Save Report" under the "File" menu, for later consult. Each of the graphics produced can also be saved in a variety of picture formats using the saving option available in the toolbar present in each of the graphics.

Another alternative to perform HRV analysis relies on the use of RR intervals time
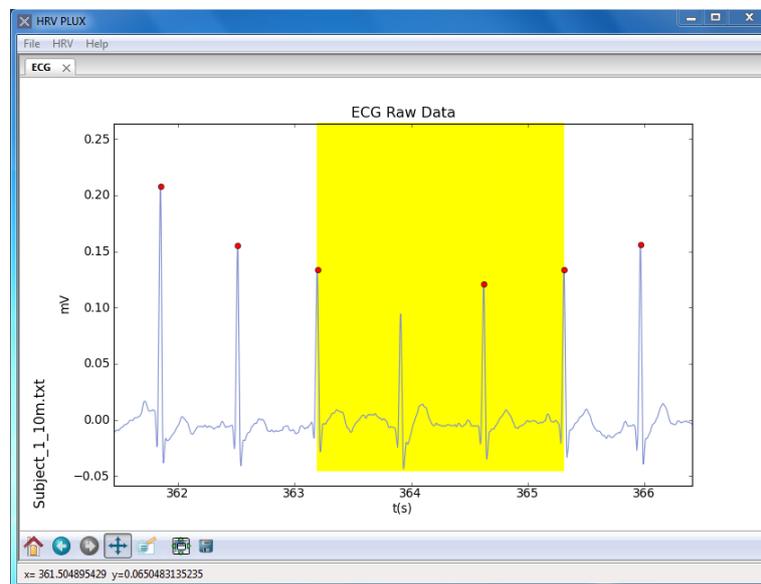
Figure 5.4: ECG signal with a R peak manually marked.
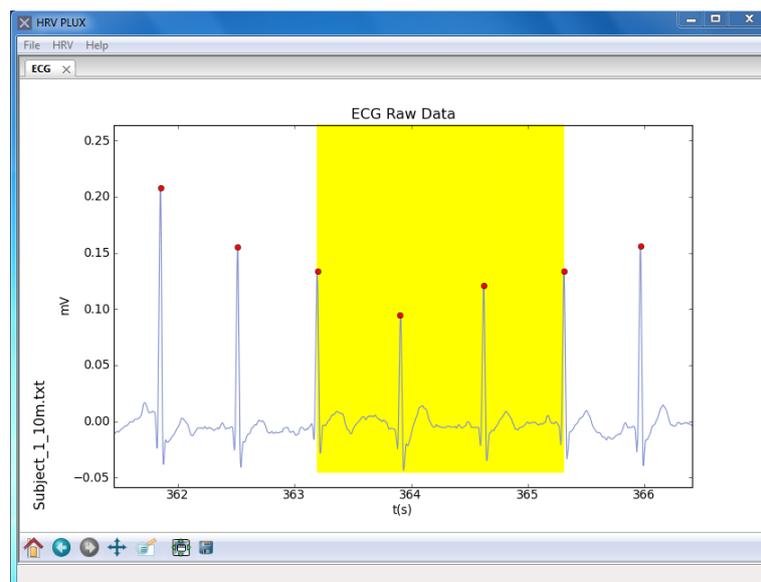
Figure 5.5: ECG signal with a R peak manually marked.
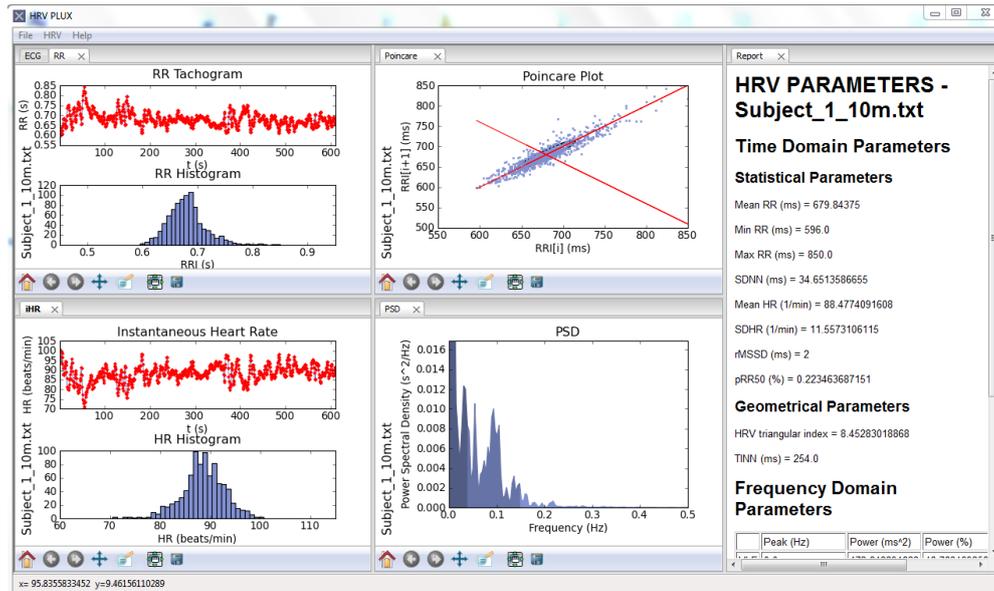
Figure 5.6: HRV analysis using an ECG signal acquired with a *bioPLUX research system*.

series directly. These intervals can be computed by a few number of ECG analysis softwares (e.g. *AcqKnowledge* [35]). This functionality is also available in our software. The user can save the intervals after any ECG or PPG HRV analysis, using the "Save RR intervals" option, and these intervals can be used in the same session or in a future session to produce HRV analysis. The results (i.e. the report and graphics) can be saved using the procedures described above.

The toolbars present in each of the graphics are a useful feature that was adapted from the ones present in the Matplotlib graphics. It permits an easy interaction with the graphics produced, allowing to zoom in and out, move and even modify the size of the graphics. We also introduced some key shortcuts to move the ECG signals and PPG signals in the graphics, enhancing the manual edition of peaks.

5.2   User interface main features

5.2.1   Input format of data

Initially, the software was designed to work only with ECG signals, acquired with an ECG triode placed at the V2 precordial lead linked to a *bioPLUX research system*, and with RR intervals time series derived from the ECG signals and saved in a one column *ASCII text (.txt)* file.
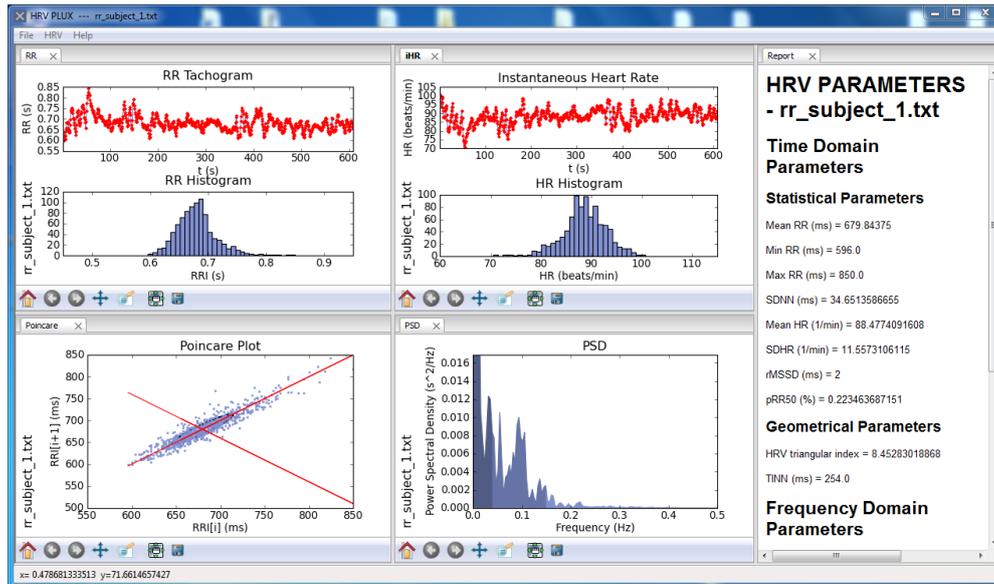
Figure 5.7: HRV analysis using RR intervals directly.

Later, the software was redesigned to support also PPG signals, once they are thought to be an effective alternative to ECG in HRV analysis. To acquire PPG signals, we used also a *bioPLUX research system* [21] with a PPG transmittance finger prototype probe attached to it.

The *bioPLUX* device can record, with a maximum sampling frequency of 1000 Hz, up to height different signals at the same time in a single *ASCII text (.txt)* file. Each one of the signals is digitalized with a 12 bit Analog-to-Digital Converter (ADC) and saved in a column of the file, corresponding to the channel used to attach the sensor.

Although NumPy has some functions created to load files, namely text files (e.g. *"loadtxt"*), such as the ones produced by the *bioPLUX* system, we had memory overflow problems when these files were to large. In order to solve this problem, we decided to develop our own load function that prevented these memory problems and was specifically designed to the files generated by the *bioPLUX*, allowing channel selection and subsampling of the signals. This function was integrated in our GUI HRV tool.

5.2.2 Peak detection

Accurate detection of ECG R and PPG peaks times is the first and crucial step in HRV analysis. In order to accomplish this task, we needed to implement precise peak detection algorithms for both signals as well as noise removing steps.

If for the ECG signals there are a wide variety of detection algorithms available,

for the PPG signals this is not true and so we had to develop our own algorithm.

Preprocessing of the signals

ECG and PPG signals are often affected by different types of noise that may interfere in the accurate R and systolic peak detection. To avoid that, at least in part, we decided to implement a few preprocessing steps that are able to remove part of that noise, leading to a better signal-to-noise ratio and a better peak detection.

In the ECG case, we have implemented an Infinite Impulse Response (IIR) 2th order butterworth low pass filter (available in SciPy library) with a 30 Hz cutoff frequency, able to remove the high frequency noise due to power line and other electronic devices interference. We also implemented an IIR 2th order butterworth high pass filter with a 2 Hz to remove baseline fluctuations due to respiration, preserving the interesting ECG frequency components. In the PPG case, since the band of interest is a little more restrict, we have implemented the low pass filter previously described with a cutoff frequency of 16 Hz that can also remove the high frequency power line interference and the interference of other electronic devices.

ECG peak detection

This section presents the algorithm implemented in our HRV GUI to detect R peaks and the correspondent occurrence time instants. The accurate detection of R peaks is the starting point for RR intervals computation and for the analysis of time oscillations between consecutive RR intervals.

The chosen algorithm is based in the Pan and Tompkins algorithm with some modifications and is a simple but effective algorithm consisting of three main components: a signal transformation, an adaptive thresholding and a local search [36, 37].

Initially, in the signal transformation phase, the filtered ECG signal is differentiated in order to accentuate the existent wave slopes. As it was described in Chapter 1, the R peak is normally the higher among all peaks in the entire ECG cycle and, consequently, will have a large slope. Since, in practical application, the signal polarity can be inverted, it has to be squared, in order to preserve the R peaks information and also to enhance its extraction. The differentiated and squared signal is then integrated within a moving window which gives a measure of how energy is distributed in the signal along

time, helping in R peak detection [36, 37].

After the transformation step, an adaptive threshold, corresponding to a fraction of the differentiated signal in each moment, is established, and a local search for peak candidates, between the points where the integrated signal crosses the threshold, is performed. As a result of the properties of cardiac tissues, every time a peak is detected a refractory period of 200 ms is initiated, where the search for a new peak is disabled.

PPG peak detection

In the previous chapter we referred that PPG signals were investigated, with success, as an alternative to ECG to derive RR intervals and therefore to study HRV. In order to implement its use in our tool, we had to develop an algorithm that was able to accurately detect local maxima of the PPG signals corresponding to the systolic peaks.

The developed algorithm has three main features: a windowed and weighted Slope Sum Function (SSF), an adaptive threshold [38] and a backsearch routine. The SSF is designed to enhance the upslope of PPG signal preserving the peaks' information. It is defined by Equation 5.1, where w is the length of the analyzing window (in this algorithm $w = 150$ ms) and $\Delta y_k = y_k - y_{k-1}$, where y_k is the PPG signal at the instant k [38].

$$z_i = \sum_{k=i-w}^{i} \Delta u_k, \ \Delta u_k = \begin{cases} \Delta y_k, & \text{if } \Delta y_k > 0 \\ 0, & \text{if } \Delta y_k < 0 \end{cases} \tag{5.1}$$

After the SSF as been applied to the signal, the search for systolic peaks is initiated using an adaptive threshold and a decision criteria. At the beggining, since there is no peak detected, the threshold is initialized at three times the mean of the first ten seconds of the PPG signal. A local search is performed in order to find the maximum between the points where the threshold crosses the SSF, which correspond to the first systolic peak. Every time a peak is detected, the threshold is adaptively updated, based on the value of the previous peak.

In some situations, where the decays between consecutive systolic peaks are too large, the peak detection may fail. In order to overcome this problem, we had to introduce a backsearch routine to avoid the loss of peaks. This routine first checks for the time that has passed since the last peak detection. If this time (Δt_i) is higher then
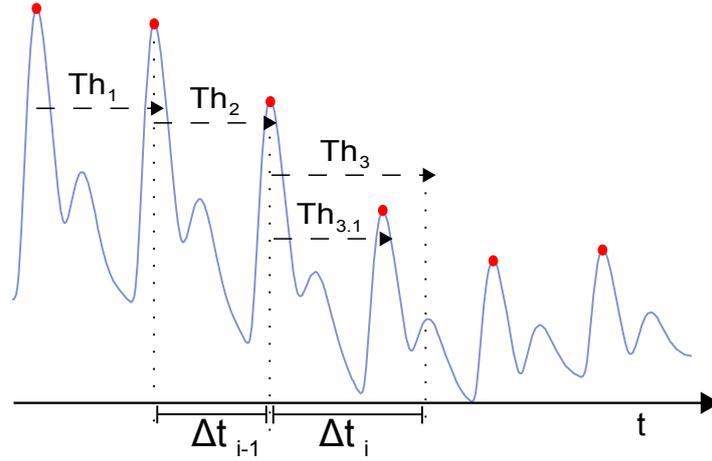
Figure 5.8: PPG backsearch routine.

110% of the previous time interval between two peaks detected (Δt_{i-1}) (i.e. Equation 5.2 is verified) the algorithm restarts the search from the last peak with a lower threshold ($Th_{3.1}$) (see Figure 5.8).

In Figure 5.8 we can see that the first two thresholds, Th_1 and Th_2, were normally established and there was no need to initiate a backsearch routine. However, the third threshold, Th_3, did not cross any peak due to its low magnitude. In this case, Equation 5.2 will be verified, the backsearch routine will decrease the threshold value to $Th_{3.1}$ and the systolic peak will now be detected.

$$\Delta t_i > 110\% \times \Delta t_{i-1} \tag{5.2}$$

5.2.3   Automatic identification of outlier intervals

In some cases, due to noise, motion artifacts or ectopic beats, the R peak detection and the systolic peak detection is not 100% effective. In order to improve the identification of skipped peaks and its location in the signal, we have implemented an automatic graphical feature that highlights, using a red band (see Figure 5.9), outlier RR intervals with more than 1.8 seconds.

In addition, since phenomena such as arrhythmias and ectopic beats, that are reflected in ECG and PPG signals, could be an important source of information to the physicians, we also implemented a method to identify abnormal patterns that follow Kammath *et. al* [39] suggestions. Kammath argues that, in sinus rhythm, each RR interval should not increase more than 32.5% or decrease more than 24.5% relatively
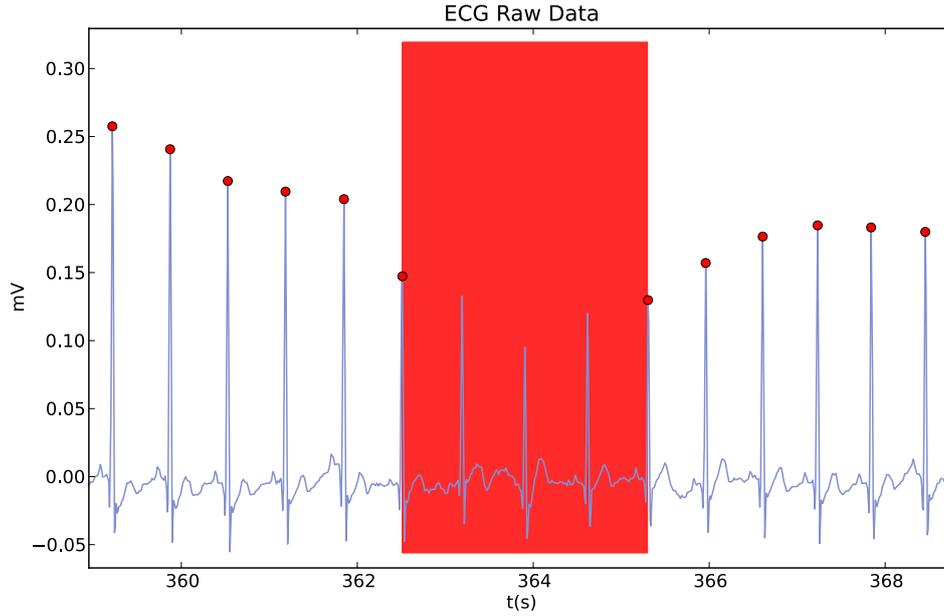
Figure 5.9: ECG with the skipped peaks highlighted.

to the previous interval. These patterns are identified with yellow bands (see Figure 5.4).

5.2.4 Manual edition of peaks

The possibility of manually editing the peaks detected by the software was implemented in our GUI as a complement of the automatic detection of outlier intervals. It gives the physician the possibility to remove, add or change a peak of place with only a simple click with the mouse (see Figure 5.5).

This functionality took advantage of the capabilities given by the Matplotlib library.

5.2.5 RR intervals time series derivation

Derivation of RR intervals is a fundamental but simple task that consists in computing the time intervals between consecutive peaks. It can be performed after the peaks have been detected and the signal manually inspected to correct, if necessary, skipped or wrongly marked peaks. In our algorithm, this is simply achieved by computing the first order difference of the R peaks or systolic peaks times array (Equation 5.3, where $1 < j < N - 1$ and N is the total number of peaks).

$$RR_j = R_{j+1} - R_j \tag{5.3}$$

Chapter 6

Experimental Results

In the previous chapter we have described the HRV analysis GUI developed, its main features and the algorithms implemented to detect R and systolic peaks from ECG and PPG signals, respectively. In this chapter, the methods and results from three different studies that we have performed, regarding these topics, will be presented.

In first place, we carried out a study to validate the algorithms implemented in our HRV GUI using the standard signals: the ECG signals. Then, in a second study, we evaluated the sensitivity and specificity of the algorithm developed to detect local maxima of PPG signals. The last study had the purpose to investigate the correlation between HRV parameters calculated from both ECG and PPG signals.

6.1   Signals Database

In order to perform the three studies mentioned above we collected a set of PPG and ECG signals from nineteen healthy subjects with ages between 17 and 53 years old. It is important to note that not all the subjects and types of signals were used in the three studies. In the first study (Section 6.3) we used only ECG signals from eighteen of the nineteen subjects, whereas in the second study (Section 6.4), we used the entire set of data and, finally, in the last study (Section 6.5), we used both ECG and PPG signals from the same eighteen subjects used in the first study. The reason for this exclusion has to do with the high rate of artifacts present in the signal collected from one of the subjects.

6.2   Signal Acquisition Scenario

The subjects were instrumented with a finger PPG sensor placed on the fourth finger
of the left hand and an ECG triode at V2 precordial lead connected to a *bioPLUX*
acquisition system. The acquisition of ECG and PPG signals was performed simulta-
neously, with the subjects seated and with their left forearm resting on an horizontal
platform.

The PPG sensor used was developed in the context of another *PLUX* project, intit-
uled "Desenvolvimento de um sensor de fotopletismografia para monitorização cardíaca
para aplicação no pulso" [40].

6.3   HRV GUI validation

The HRV GUI validation was performed following the recommendations of by J. Bland
and D. Altman for "assessing agreement between two methods of clinical measure-
ment" [41, 42]. They suggest to compare the method under validation with an estab-
lished one, following a well defined sequence of steps.

In order to follow their suggestions we decided to compare our HRV GUI with an
existing tool called Kubios HRV [43]. However, this tool has a few limitations, when
compared with our's, the most obvious one being the fact that it only accepts RR
intervals as the input data, in order to compute HRV analysis. Therefore, we first had
to compute such intervals with our GUI.

In the next subsections we present the results of the statistical study conducted to
validate our HRV GUI, by comparing it with Kubios HRV.

6.3.1   Comparison Procedure

The J. Bland and D. Altman method compares two different methods by plotting the
differences between them against their mean. We have applied this method for ten
different HRV parameters and computed the "limits of agreement" as suggested. The
limits correspond to the mean of the differences plus/minus two times the standard
deviation (i.e. MEAN +/- 2SD and MEAN - 2SD). If this limits are low enough, when
compared with the mean values, we can decide that our tool is a valid alternative to
compute HRV analysis.

6.3.2 Results and discussion
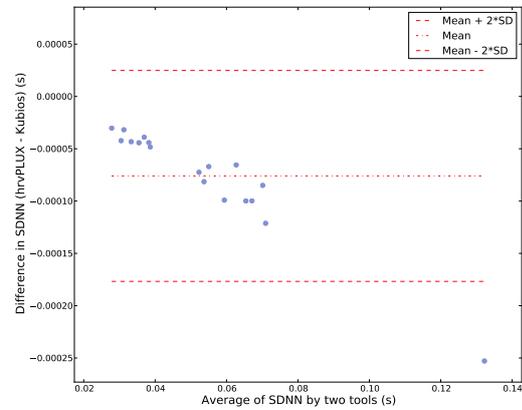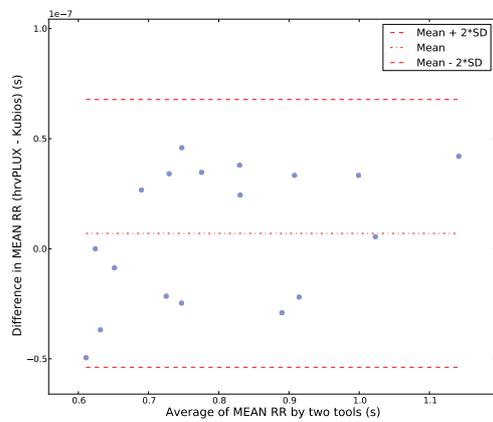
(a) Average of RR intervals in both ECG and PPG signals.

(b) SDNN of RR intervals in both ECG and PPG signals.
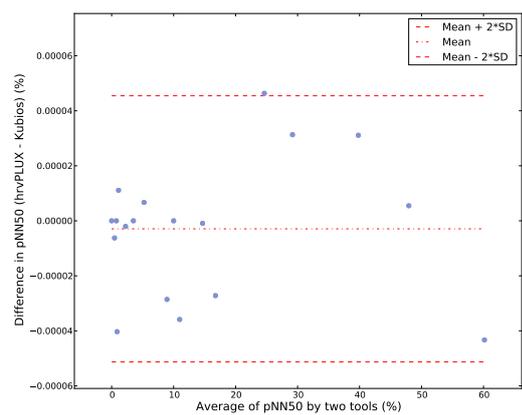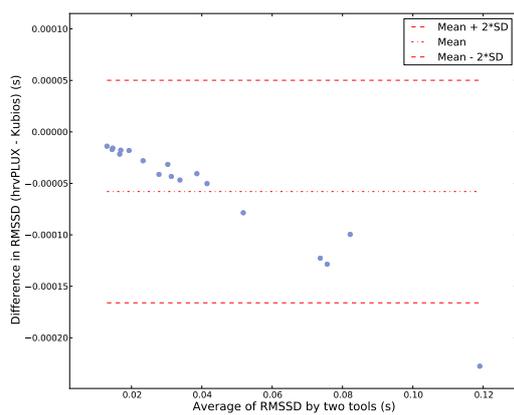
(c) RMSSD of RR intervals in both ECG and PPG signals.

(d) pNN50 of RR intervals in both ECG and PPG signals.

Figure 6.1: Results from the Bland and Altman's comparison analysis of time domain HRV parameters.
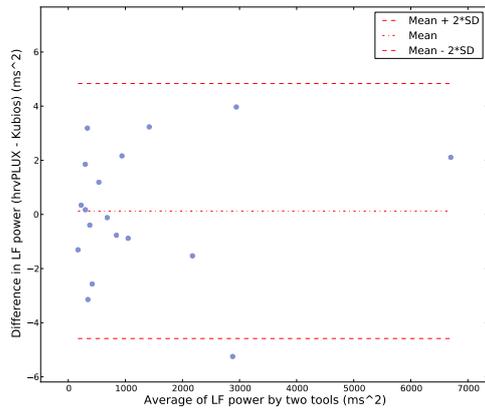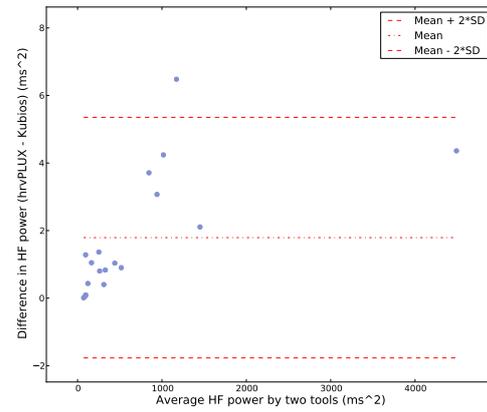
(a) Absolute LF power.

(b) Absolute HF power.
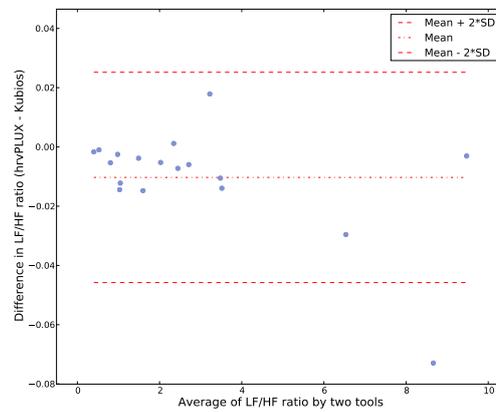
(c) Ratio between LF and HF band powers.

Figure 6.2: Results from the Bland and Altman's comparison analysis of frequency domain HRV parameters.
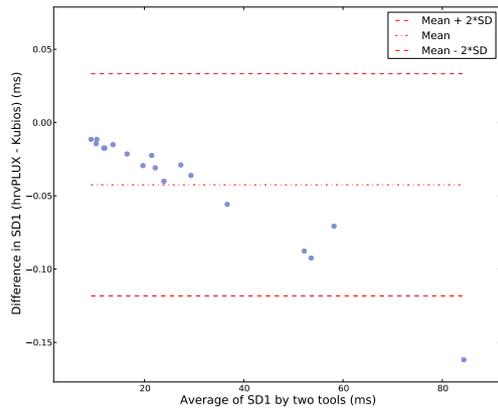
(a) SD1.
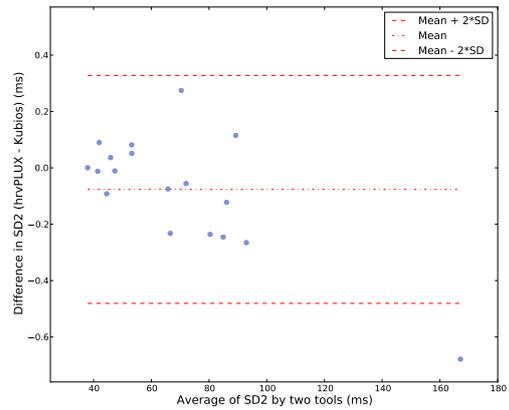
(b) SD2
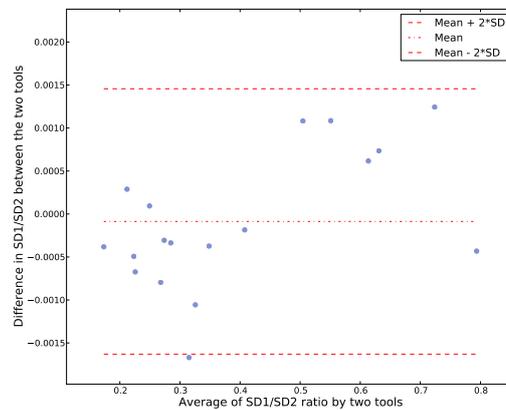
(c) SD1/SD2 ratio.

Figure 6.3: Results from the Bland and Altman's comparison analysis of nonlinear HRV parameters.

The graphics presented in Figures 6.1, 6.2 and 6.3 show the results for the Bland and Altman analysis, performed to validate the HRV GUI developed.

From the analysis of such graphics we can observe that, for the ten HRV parameters compared, the differences between the two methods were always smaller than 1% of the means, even in the worst case scenarios. Although three of the graphics (Figures 6.1(b), 6.1(c) and 6.3(a)) show a clear trend as the means values increase, which can mean that something is influencing the results. Nevertheless, we can say that the differences and the limits of differences are small enough for us to be confident that our method can be used in alternative to Kubios HRV.

Despite these results we suggest further studies with more subjects to understand and mitigate such trends, that are influencing this study.

6.4 PPG peak detection sensitivity and specificity study

This section describes the methods implemented and the results obtained for the sensitivity and specificity study of the developed PPG peak detection algorithm (see also Subsection 5.2.2). This algorithm is the starting point for another study conducted in order to verify that the PPG signals can be used as an alternative to ECG for HRV analysis purposes.

6.4.1 Evaluation Procedure

The procedure used to determine the number of true positives, false positives, true negatives and false negatives, necessary for Equations 6.1 and 6.2, to assess sensitivity and specificity of two versions of our algorithm (one with a backsearch routine and another without this routine), is based on the comparison of the detected peaks in the PPG signal with the number of ECG peaks previously annotated. The peaks were checked by visual inspection whenever a critical point (i.e. a point where the detection has probably failed) was detected.

$$\text{sensitivity} = \frac{\text{nr of true positives}}{\text{nr of true positives} + \text{nr of false negatives}} \tag{6.1}$$

$$\text{specificity} = \frac{\text{nr of true negatives}}{\text{nr of true negatives} + \text{nr of false positives}} \tag{6.2}$$

The search for critical points followed two different approaches. In the first approach, we compared the number of maxima in the PPG signal with the number of ECG peak annotations, and if they were equal, we checked whether there were discrepancies in the intervals between consecutive peaks in both PPG and ECG signals. When discrepancies were found, they were marked as critical points and visually inspected to understand if they corresponded or not to lost peaks in the PPG signal. In the second approach, if the number of maxima in the PPG signal was different from the number

of ECG peak annotations, we had to perform a visual inspection to find critical points, since time intervals could not be compared directly.

6.4.2 Results and discussion

Table 6.1: Sensitivity and specifity results of the algorithm with the backsearch routine.

	Sen (%)	Spe (%)
Gross	99.94	100
Average	99.93	100

Table 6.2: Sensitivity and specifity results of the algorithm without the backsearch routine.

	Sen (%)	Spe (%)
Gross	99.60	100
Average	99.58	100

As to the sensitivity and specificity of the two different versions of our algorithm, developed to detect PPG maxima (i.e. PPG systolic peaks) we can see from Tables 6.1 and 6.2, that the version with backsearch routine showed a gross sensitivity of 99.94% for all the peaks annotated in the ECG signals and an average sensitivity of 99.93%, while the other version showed 99.60% and 99.58%, respectively. Regarding gross and average specificity, both versions presented a 100% score. Therefore, the results obtained for our algorithm showed high levels of sensitivity and specificity, specially in the version with the backsearch routine.

This study was also important as it showed that physiological phenomena such as PVC, that are normally seen in ECG signals, are also be observed in the PPG ones. This situation highly affected the algorithm's sensitivity and has been the cause of most of non detected peaks, since in most of the situations it leads to attenuation or complete suppression of PPG pulses.

6.5 Correlation study between HRV derived from both PPG and ECG signals

In Chapter 4 we have discussed the use of PPG signals as an alternative to ECG, and the possibility of using them in our tool. In this section we present a correlation study,

that took advantage of the algorithm described in the previous section, in order to analyze and validate such alternative.

6.5.1   Correlation Analysis

The correlation between the HRV parameters calculated from PPG and ECG signals was estimated by performing linear regression analysis for each of the parameters using data collected from eighteen subjects. This analysis returns the *Pearson correlation coefficient* and its square (i.e. *coefficient of determination*), r and R^2, respectively.

6.5.2   Results and discussion
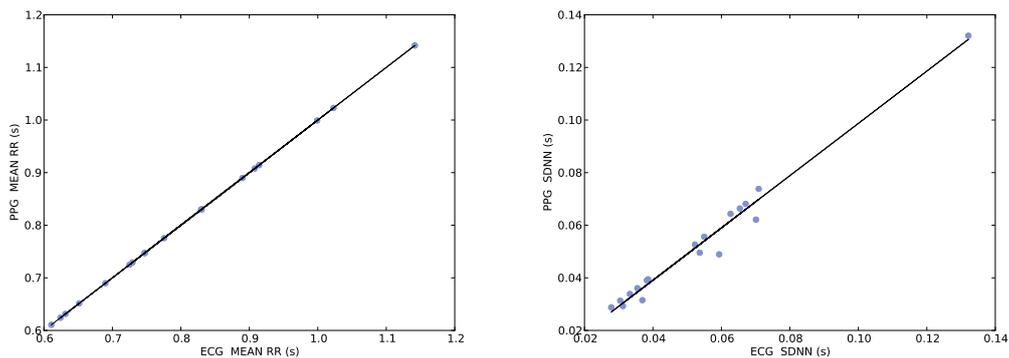
(a) Average of RR intervals in both ECG and PPG signals.

(b) SDNN of RR intervals in both ECG and PPG signals.
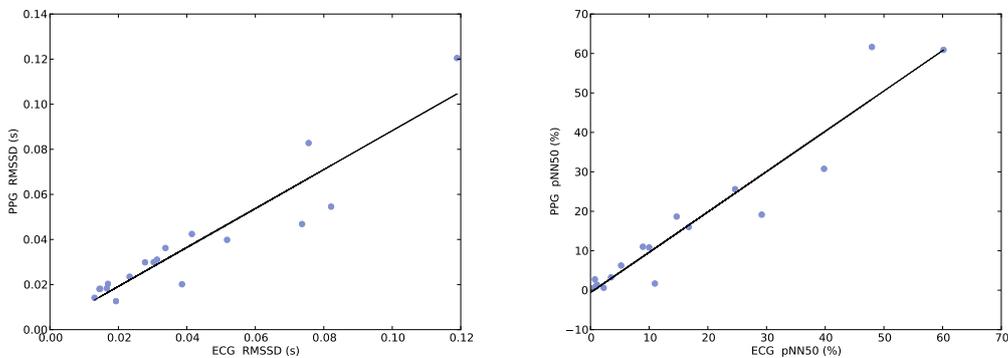
(c) RMSSD of RR intervals in both ECG and PPG signals.

(d) pNN50 of RR intervals in both ECG and PPG signals.

Figure 6.4: Linear regression analysis of time domain HRV parameters.
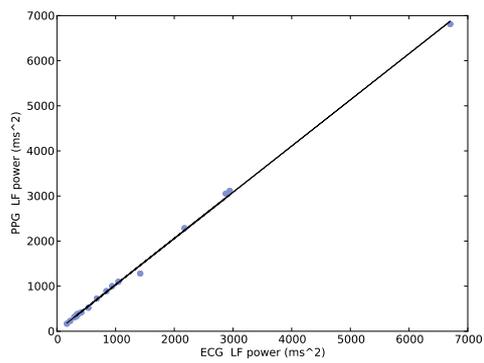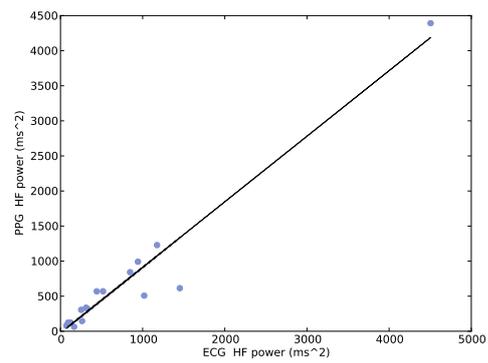
(a) Absolute LF power.   (b) Absolute HF power.
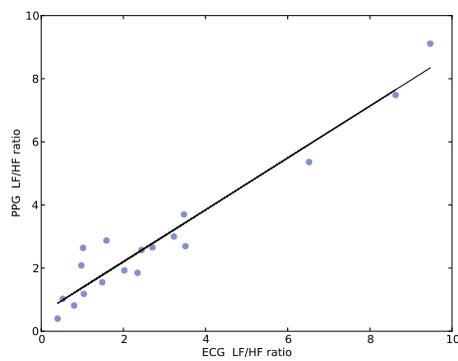
(c) Ratio between LF and HF band powers.

Figure 6.5: Linear regression analysis of frequency domain HRV parameters.

(a) SD1.   (b) SD2

(c) SD1/SD2 ratio.
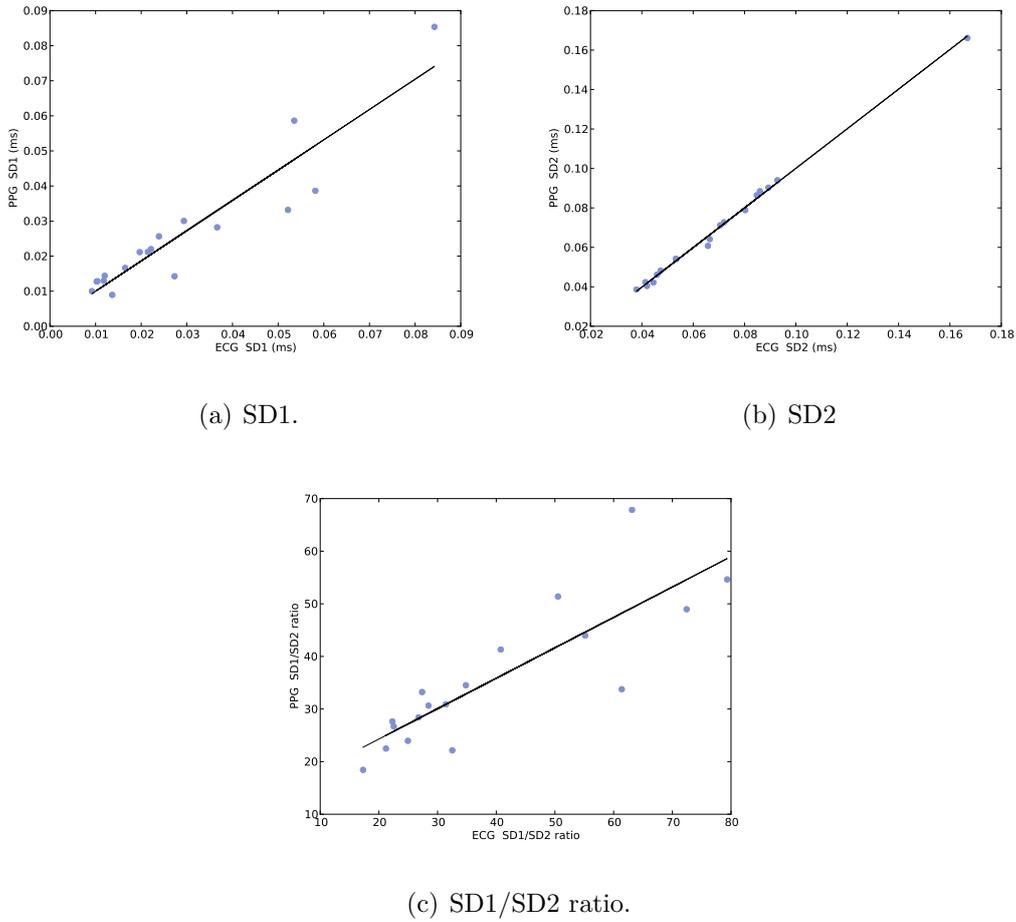
Figure 6.6: Linear regression analysis of nonlinear HRV parameters.

Table 6.3: r and R^2 results for time domain parameters.

	MEAN RR	SDNN	RMSSD	pNN50
r	1.000	0.989	0.934	0.961
R^2	1.000	0.979	0.872	0.923

Table 6.4: r and R^2 results for frequency domain parameters.

	LF POWER	HF POWER	LF/HF RATIO
r	0.999	0.974	0.967
R^2	0.997	0.949	0.935

Table 6.5: r and R^2 results for nonlinear parameters.

	SD1	SD2	SD1/SD2 RATIO
r	0.934	0.998	0.840
R^2	0.872	0.997	0.706

The results obtained for the linear regression and correlation analysis of the HRV parameters are showed in Figures 6.4, 6.5, 6.6 and in Tables 6.3, 6.4, 6.5.

Analyzing Tables 6.3, 6.4, 6.5 we can observe that the parameter with the highest *Pearson coefficient* was the *MEAN RR* which means that it shows, as expected, the best correlation among the parameters analyzed. On the other hand the parameter with the smallest *r value* and consequently showing the worst correlation was the *SD1/SD2 RATIO*. The best correlation results were obtained for the frequency domain analysis parameters, which means that among the three categories of parameters computed, these were the ones that showed the highest correlation with the same parameters derived from the ECG signals.

This study revealed high correlation when comparing the HRV parameters calculated using signals from both sensors. However, some limitations such as the presence of motion artifacts in the PPG signal were identified. In order to avoid noise caused by motion we suggest signal acquisition to be performed in controlled scenarios and the introduction, in the future, of adaptive filtering strategies to remove it.

The current study strongly suggests that PPG signals can be used as a good alternative to derive HRV parameters and to understand the dynamic under the ANS. This conclusion is in agreement with earlier studies already mentioned.

Chapter 7

Conclusions

As have been described along this work, HRV has an enormous potential to assess the role of ANS at the cardiovascular level, in normal healthy individuals, as well as, in patients with different disorders.

The main goal of this work was to develop an easy to use and full featured GUI, with accurate algorithms, able to compute automatic HRV analysis using ECG signals acquired with a *bioPLUX acquisition system* and an *ecgPLUX sensor*.

During the initial phase of the work, new possibilities for HRV extraction, based in PPG signals, have been investigated and, as a result, additional goals were established. The new goals consisted in, firstly, develop an algorithm able to accurately detect the systolic peaks in PPG signals and, secondly, to implement an alternative way to compute HRV analysis, using the new algorithm and PPG signals collected with a sensor, that was being developed at *PLUX, Lda*.

Until the end of this work, we were able to produce a Python based cross platform GUI, provided with powerful algorithms, capable to easily compute HRV analysis using ECG signals, PPG signals and also RR intervals. Through the developed GUI, the user can effortlessly inspect the signal for abnormal situations (e.g., peaks skipped by the algorithm and abnormal RR intervals) and, in same cases, correct them interactively. The user can also save reports that can be used for future analysis.

Additionally, we have performed three different studies, reported in Chapter 6, in order to investigate the validity of our developments.

Despite all the progresses that have been accomplished with this project, we feel that there are still many possibilities to explore. As so, we suggest, as possible directions

to follow, the implementation of new parameters, specially derived from nonlinear methods; the study of specific pathologies, such as the ones described in Chapter 3, with the developed GUI; and to investigate the use of HRV in biofeedback protocols [25].

Finally, and taking into account the developed work, we can say, as a final consideration, that the main goals that have been purposed were achieved with success.

Appendix A

Publications

A.1   TMSi 2010

Blood Volume Pulse Peak Detector with a Double Adaptive Threshold

J. Medeiros & R. Martins,
Departamento de Física, Faculdade de Ciências e Tecnologia, Universidade de Coimbra, Coimbra, Portugal

S. Palma[1] & H. Gamboa[1,2]
[1]PLUX – Wireless Biosignals, Lisboa, Portugal

[2]CEFITEC – FCT – Universidade Nova de Lisboa, Lisboa, Portugal

M. Reis,
Departamento de Engenharia Química, Faculdade de Ciências e Tecnologia, Universidade de Coimbra, Coimbra, Portugal

ABSTRACT: Blood Volume Pulse (BVP) signal processing is a method to access heart rate and other cardiovascular parameters. In this work we developed an algorithm that detects the cardiac systole from the BVP signal with high accuracy. The implemented algorithm consists of a slope sum function (SSF), an adaptive threshold strategy and a backsearch routine which works as a double adaptive threshold to enhance the sensitivity of the systole detection. In order to evaluate the performance of our algorithm we synchronously acquired BVP and eletrocardiogram (ECG) signals from a group of nineteen volunteers. The QRS complexes were annotated in the ECG signals and used as reference to detect false positives and false negatives in BVP detected systoles. The algorithm detected 99.94% of the 20 210 BVP systoles evident.

Keywords: blood volume pulse sensor, pulse detector, adaptive threshold, backsearch routine, algorithm, signal processing.

1 INTRODUCTION

The BVP signal is obtainned with a photoplethysmography sensor. This sensor measures the changes in blood flow in arteries and capillaries during the cardiac cycle by shinning an infrared light-emission diode (LED) through the tissues (Peper et al. 2007 and Webster 1997). The intensity of light that travels through the tissue and is detected in the photodetector changes proportionally to the amount of blood flowing in the tissues (Haahr 2006).

Since the BVP signal reflects the blood changes that occur during a cardiac cycle it can be used as an alternative to ECG to assess instantaneous heart rate and the rr intervals. Some of the advantages of using a BVP sensor to extract the referred parameters are the fact that the sensor is non-invasive and is less obstrusive than an ECG sensor (Peper et al. 2007). Additionally, it is possible to extract from this signal other parameters, such as pulse transit time and peripheral vasodilatation (Reisner et al. 2008).

In the following sections we describe the development of an automated algorithm for detection of local maxima of the BVP pulses, which correspond to systoles in the cardiac cycle. An accurate detection of this parameter in the BVP signal is important for the computation of variables used to access the subject's health condition, such as heart rate variability (Haarh 2006; Reisner et al. 2008). Applications of this sensor and algorithm in health care range from internship and ambulatory healthcare to long-term patient monitoring. (Peper et al. 2007).

2 METHODS

2.1 *The Algorithm*

We implemented an algorithm that detects the local maxima of BVP pulses. The algorithm consists in three main steps: a slope sum function (SSF), an adaptive threshold (Zong 2003) and a backsearch routine.
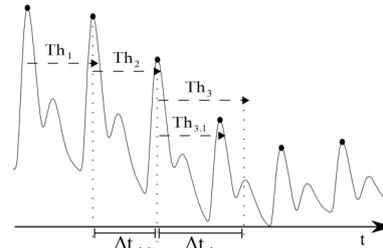

Figure 1. BVP signal with a regular pulse detection and with a backsearch pulse detection

When applied to the BVP signal, the SSF allows to keep pulses' information. The signal that results from the SSF is, then, checked for local maxima using an adaptive threshold and a deci-

sion criteria to determine whether or not a maximum occurs in each SSF pulse (Zong 2003).

When a maximum is detected, the threshold (Th) is updated according to the value of that maximum. For each SSF pulse, the algorithm performs a local search for its maximum value between the two points where the threshold is crossed.

In order to avoid the loss of maxima due to big decays in the value of the maximum between consecutive BVP pulses, we implemented a backsearch routine. When (1) is verified the backsearch is activated and a lower threshold ($Th_{3.1}$) is set (Figure 1).

$$\Delta t_i > 110\% \times \Delta t_{i-1} \tag{1}$$

2.2 *Database and Acquisition Scenario*

To test the developed algorithm we collected a set of data composed of BVP and ECG from nineteen healthy volunteers with ages between 17 and 53 years old. Each volunteer was instrumented with a finger BVP sensor placed on the 4th finger of the left hand and an ECG triode at V2 precordial lead connected to a *bioPLUX research* data acquisition system (PLUX 2010). The acquisition of ECG and BVP signals was performed synchronously, with the subjects seated and with their left forearm resting on an horizontal platform. The data collected along with the correspondent ECG QRS annotations is available on the Open Signals database (http://www.opensignals.net).

2.3 *Algorithm Evaluation Procedure*

The method used to assess the accuracy of the algorithm is based on the comparison of the number of maxima detected in the BVP signal with the number of ECG pulse annotations. The comparison was performed by visual inspection when a critical point was detected. To find a critical point we used two different approaches. In both approaches we verified if the number of maxima detected in the BVP signal was the same as the annotated in the correspondent ECG.

In the first approach, if the number of maxima in the BVP was equal to the number of ECG pulse annotations, we checked if there were some discrepancies in the time intervals between consecutive maxima in both BVP and ECG. The discrepancies were identified as critical points and visually inspected in order to decide if they corresponded or not to lost maxima in the BVP signal.

In the second approach, if the number of of maxima in the BVP was different from the number of ECG pulse annotations, we had to visually inspect the signal and look for critical points because we could not compare the time intervals directly.

We have applied this method to determine the number of true and false positives as well as true and false negatives, which will be used to evaluate the sensitivity and specificity of two versions of the algorithm: (a) with backsearch routine and (b) without backsearch routine.

3 RESULTS AND DISCUSSION

Sensitivity and specifity results of the two versions of the algorithms are listed in table 1 and 2.

Tabel 1. Sensitivity and specificity of the algorithm with the backsearch routine

	Sen (%)	Spe (%)
Gross	99.94	100
Average	99.93	100

Tabel 2. Sensitivity and specificity of the without the backsearch routine

	Sen (%)	Spe (%)
Gross	99.60	100
Average	99.58	100

The version with backsearch routine presents a sensitivity of 99.94% for the 20 210 peaks annotated in the ECG while the second version showed a sensitivity of only 99.60% for the same dataset. On the other hand, specificity was 100% for both versions.

Analyzing these results it is valid to induce that our strategy revealed high levels of performance and that the backsearch routine increased the sensitivity of the algorithm.

Our study also revealed that the algorithm's sensitivity is highly affected by physiological phenomena like Premature Ventricular Contraction (Keany and Desai 2010) which can lead to attenuation and suppression of some BVP pulses. This situation has been the cause of most of non-detected BVP pulses.

Excluding those events we can conclude that the present algorithm showed an excellent performance.

REFERENCES

Haahr, R., 2006. Reflectance Pulse Oximetry Sensor for the Electronic Patch. Technical University of Denmark.

Keany, J.E. & Desai, A.D., Premature Ventricular Contraction: eMedicine Emergency Medicine. Available at: http://emedicine.medscape.com/article/761148-overview [Accessed May 13, 2010].

Peper, E. et al., 2007. Is There More to Blood Volume Pulse Than Heart Rate Variability, Respiratory Sinus Arrhythmia, and Cardiorespiratory Synchrony? Biofeedback, 35(2), 54-61.

PLUX, bioPLUX Research. PLUX Wireless Biosignals. Available at: www.plux.info [Accessed April 5, 2010].

Reisner, A. et al., 2008. Utility of the Photoplethysmogram in Circulatory Monitoring. Anesthesiology, 108(5), 950-958.

Webster, J.G., 1997. Design of pulse oximeters, IOP Publishing Ltd.

Zong, W. et al., 2003. An Open-source Algorithm to Detect Onset of Arterial Blood Pressure Pulses. *Computers in Cardiology*, 30, 259-262.

A.2   IBERSENSOR 2010

Development of a Blood Volume Pulse Sensor to measure Heart Rate Variability

R. Martins & J. Medeiros,

Departamento de Física, Faculdade de Ciências e Tecnologia, Universidade de Coimbra, Coimbra, Portugal

S. Palma[1] & H. Gamboa[1,2]

[1]PLUX – Wireless Biosignals, Lisboa, Portugal

[2]CEFITEC – FCT – Universidade Nova de Lisboa, Lisboa, Portugal

M. Reis,

Departamento de Engenharia Química, Faculdade de Ciências e Tecnologia, Universidade de Coimbra, Coimbra, Portugal

ABSTRACT: Biomedical systems to access physiological signals are, nowadays, in great development. In this context, non-invasive and more user-friendly methods play a role of leading impact in clinical as well as in research activities. The blood volume pulse (BVP) sensor is an example of a much more practical and easy to use method to access some cardiac variables than the electrocardiography (ECG) sensor. With the appropriate data processing algorithms, it allows the access to heart rate (HR) and heart rate variability (HRV) parameters. In the present work we developed a BVP sensor with the aim of obtaining a signal from which HRV parameters can be computed with high reliability. We acquired simultaneously BVP and ECG signals from a group of subjects and used an offline processing algorithm to compute HRV parameters from both signals. This study has shown a strong positive association between all the parameters calculated using BVP and ECG signals.

1 INTRODUCTION

The heart rate variability is an indirect measure of the activity of the autonomous nervous system and the sympathovagal balance, since heart rate is controlled by the sinoatrial node [1, 2]. It has already been proved that the analysis of HRV allows to stratify the risk after myocardial infarction and to early detect diabetic neuropathy [3, 4]. HRV describes the changes in the time intervals between successive heartbeats. Therefore, the accurate detection of heart beats' timing is of crucial importance for the HRV analysis. This detection is, generally, accomplished using the ECG signal. Nevertheless, BVP signals seem to be a very promising alternative [3, 5].

BVP sensors can be used to detect heart beats, based on a principle called photopletysmography (PPG) which consists of measuring the changes in volume using an optical method. In the particular case of BVP sensors, that measure the amount of infrared light absorbed by the blood, the changes in volume are caused by variations in blood pressure in the vessels occurring during each cardiac cycle [6, 7].

Compared with an ECG sensor, the BVP sensor has some advantages, namely it is more 'user friendly' and less obtrusive. However, since the BVP signal is affected by motion artifacts the measurements have to be performed in controlled environments. In order to evaluate the correlation between the HRV parameters computed from a BVP and ECG signals acquired simultaneously, we developed a BVP sensor to use with a *bioPLUX research* [8] system.

2 METHODS

2.1 *Acquisition system architecture*

The developed system consists in a two module BVP sensor and a signal acquisition module, as illustrated in Figure 1. The signal is acquired by the reception module of the BVP probe and conditioned by a filtering and an amplification stage. The analog signal to digital conversion and bluetooth transmission to the computer is performed using a *bioPLUX research* [8] signal acquisition system.
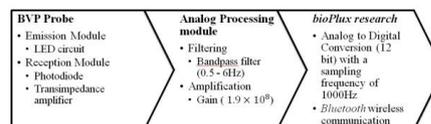

BVP Probe	Analog Processing module	*bioPlux research*

• Emission Module
  • LED circuit
• Reception Module
  • Photodiode
  • Transimpedance amplifier
	• Filtering
	  • Bandpass filter (0.5 - 6Hz)
	• Amplification
	  • Gain (1.9×10^8)
		• Analog to Digital Conversion (12 bit) with a sampling frequency of 1000Hz
		• *Bluetooth* wireless communication

Figure 1. System architecture

2.2 *HRV algorithm*

The HRV analysis algorithm and all the digital signal processing involved in the present work was performed using custom developed Python routines (with SciPy and Numpy modules). ECG and BVP data was acquired using a *bioPLUX research* [8] system. The developed HRV algorithm follows the standards suggested by a previously published guideline [9].

In order to perform the HRV parameters' calculus, the algorithm first accesses the QRS complexes and local maxima of BVP pulses for the first 5 minutes of ECG and BVP signals, respectively. The second step consists of the calculus of R-R intervals in the ECG signal and in-

terbeat intervals in the BVP signal. HRV parameters (Table 1) are, then, computed using these values.

Table 1. HRV parameters calculated

Time Domain	Frequency Domain	Nonlinear
Mean NN (mean interbeat interval)	HF (High Frequency power)	SD1 (Short-term variability)
SDNN (standard deviation of interbeat interval)	LF (Low Frequency Power)	SD2 (Long-term variability)
RMSSD (square root of the mean squared difference of successive interbeat intervals)	LF/HF ratio	SD1/SD2 ratio
pNN50 (differences of successive interbeat interval greater than 50 ms divided by the total number of intervals)		

2.3   *Correlation Analysis*

The similarity of the HRV parameters calculated from BVP and ECG signals was assessed by performing linear regression analysis. Linear regression analysis returns the Pearson correlation coefficient and its square, r and R^2, respectively.

2.4   *Dataset and Acquisition Scenario*

To test our algorithm we collected a set of data composed of BVP and ECG signals, with variable lengths, from eighteen healthy volunteers with ages between 17 and 53 years old. Each volunteer was instrumented with our BVP sensor prototype placed on the 4th finger of the left hand and an ECG triode at V2 precordial lead connected to a *bioPLUX research* [8] data acquisition system. The acquisition of ECG and BVP signals was performed synchronously, with the subjects seated and with their left forearm on an horizontal platform. The data collected along with the correspondent ECG QRS complex annotations was made available on the Web in the Open Signals database (http://www.opensignals.net).

3   RESULTS AND DISCUSSION

The results obtained for the linear regression analysis of the HRV parameters are listed in Table 2, 3, 4.

Table 2. r and R^2 results for time domain parameters

	MEAN NN	SDNN	RMSSD	pNN50
r	1.000	0.989	0.934	0.961
R^2	1.000	0.979	0.872	0.923

Table 3. r and R^2 results for frequency domain parameters

	LF POWER	HF POWER	LF/HF RATIO
r	0.999	0.974	0.967
R^2	0.997	0.949	0.935

Table 4. r and R^2 results for nonlinear parameters

	SD1	SD2	SD1/SD2 RATIO
r	0.934	0.998	0.840
R^2	0.872	0.997	0.706

Several studies point the BVP signal as an interesting alternative to ECG signal when it comes to the measurement of HRV in home care and clinical situations [3, 10].

The results obtained show that the parameters of HRV derived from our BVP sensor are highly correlated with the parameters of HRV derived from ECG.

Analyzing the results in detail we can observe that the mean NN obtained the maximum R^2 value, showing an excellent correlation between the means calculated from the two different signals. On the other hand the SD1/SD2 ratio presents the minimum R^2 value observed and, consequently, is the least correlated HRV parameter. The best R^2 values were obtained for the frequency domain analysis parameters, which means that among the three categories of parameters computed from the BVP signal analysis, the frequency domain are highly correlated with the same parameters computed from the ECG signal.

The major limitations identified for the use of the BVP sensor are motion artifacts. To avoid noise caused by motion, the BVP signal acquisition needs to be performed under a controlled scenario. Eventual modifications of the physical packaging of the sensor could mitigate the influence of these kind of artifacts.

With the present study we can conclude that the use of the BVP sensor for the HRV analysis is a legitimate alternative and gives accurate results, highly correlated with the results obtained from ECG signal processing. Thus, our results are in accordance with the mentioned studies, indicating that BVP could be used as an alternative to the ECG for HRV analysis.

REFERENCES

[1] M.P. Tarvainen, J.P. Niskanen, J.A. Lipponen, P.O. Ranta-aho, and P. Karjalainen, "Kubios HRV - A Software for Advanced Heart Rate Variability Analysis," IFMBE, 2008.

[2] C.D. Clifford, "Signal Processing Methods For Heart Rate Variability Analysis," University of Oxford, 2002.

[3] G. Lu and F. Yang, "Limitations of Oximetry to Measure Heart Rate Variability Measures," vol. 9, Sep. 2009, pp. 119-125.

[4] G.G. Berntson, T. Bigger, D.L. Eckberg, and P. Grossman, "Heart rate variability: Origins, methods, and interpretive caveats.," Psychophysiol, vol. 34, 1997, pp. 623–648.

[5] E. Peper, R. Harvey, M. I-Mei Lin, H. Tylova, e D. Moss, "Is There More to Blood Volume Pulse Than Heart Rate Variability, Respiratory Sinus Arrhythmia, and Cardiorespiratory Synchrony?," Biofeedback, vol. 35, 2007, pp. 54-61.

[6] R. Haahr, "Reflectance Pulse Oximetry Sensor for the Electronic Patch," Technical University of Denmark, 2006.

[7] J.G. Webster, Design of pulse oximeters, IOP Publishing Ltd, 1997.

[8] PLUX, "bioPLUX Research," PLUX Wireless Biosignals. Available: http://www.plux.info [Accessed April 5, 2010].

[9] Task Force of The European Society of Cardiology and The North American Society of Pacing and Electrophysiology, "Heart rate variability: Standards of measurement, physiological interpretation, and clinical use," European Heart Journal, vol. 17, 1996, pp. 354-381.

[10] S. Lu, H. Zhao, K. Ju, K. Shin, M. Lee, K. Shelley, and K.H. Chon, "Can Photoplethysmography Variability serve as an alternative approach to obtain Heart Rate Variability information?," Journal of Clinical Monitoring and Computing, 2008.

Bibliography

[1] ZooFari, "Heart diagram," Mar. 2010. [Online]. Available: http://en.wikipedia.org/wiki/File:Heart_diagram-en.svg

[2] J. Malmivuo and R. Plonsey, *Bioelectromagnetism - Principles and Applications of Bioelectric and Biomagnetic Fields.* New York: Oxford University Press, 1995.

[3] A. Atkielski, "Schematic diagram of normal sinus rhythm for a human heart as seen on ECG," 2007. [Online]. Available: http://pt.wikipedia.org/wiki/Ficheiro:SinusRhythmLabels.svg

[4] "Premature ventricular contraction," 2008. [Online]. Available: http://www.learnekgs.com/pvc.htm

[5] M. P. Tarvainen, J. P. Niskanen, J. A. Lipponen, P. O. Ranta-aho, and P. Karjalainen, "Kubios HRV - a software for advanced heart rate variability analysis," in *IFMBE*, vol. 22, Nov. 2008. [Online]. Available: http://books.google.pt/books?id=83RUrYCMXOgC&pg=PA1022&lpg=PA1022&dq=kubios+frequency+methods&source=bl&ots=SFxCDV5zsX&sig=17QuuFCcH-fmC72esCuyrKC1BPw&hl=pt-PT&ei=0YZxS7ijItHN4gbdlODICQ&sa=X&oi=book_result&ct=result&resnum=2&ved=0CBMQ6AEwAQ#v=onepage&q=kubios%20frequency%20methods&f=false

[6] T. F. of The European Society of Cardiology, T. N. A. S. of Pacing, and Electrophysiology, "Heart rate variability: Standards of measurement, physiological interpretation, and clinical use," *European Heart Journal*, vol. 17, pp. 354–381, 1996. [Online]. Available: http://eurheartj.oxfordjournals.org/cgi/reprint/17/3/354

[7] R. Haahr, "Reflectance pulse oximetry sensor for the electronic patch," Ph.D. dissertation, Technical University of Denmark, Nov. 2006. [Online]. Available: http://www.nanotech.dtu.dk/upload/institutter/mic/forskning/mems-appliedsensors/publications/master_thesis/2006%20rasmus%20gr%C3%B8nb%C3%A6k%20haahr.pdf

[8] A. Ghuran and M. Malik, "Heart rate variability - state of the art," *Cardiac Electrophysiology Review*, vol. 3, no. 4, pp. 283–285, Dec. 1999. [Online]. Available: http://dx.doi.org/10.1023/A:1009972018981

[9] G. D. Clifford, "Signal processing methods for heart rate variability," PhD thesis, Citeseer, 2002.

[10] G. D. Clifford, F. Azuaje, and P. McSharry, *Advanced Methods And Tools for ECG Data Analysis*, 1st ed. Artech House Publishers, Sep. 2006.

[11] Mosby, "Myocardium," 2008. [Online]. Available: http://medical-dictionary. thefreedictionary.com/myocardium

[12] M. Boyett and H. Dobrzynski, "The sinoatrial node is still setting the pace 100 years after its discovery," *Circulation Research*, vol. 100, no. 11, pp. 1543–1545, 2007. [Online]. Available: http://circres.ahajournals.org/cgi/doi/10. 1161/CIRCRESAHA.107.101101

[13] A. M. Katz, *Physiology of the Heart*. Lippincott Williams & Wilkins, Nov. 2005.

[14] Nobelprize.org, "The nobel prize in physiology or medicine 1924," http://nobelprize.org/nobel_prizes/medicine/laureates/1924/, Jul. 2010. [Online]. Available: http://nobelprize.org/nobel_prizes/medicine/laureates/1924/

[15] P. D. Welch, "The use of fast fourier transform for the estimation of power spectra: A method based on time averaging over short, modified periodograms," *IEEE Transactions on Audio Electroacoustics*, vol. AU, no. 15, pp. 70–73, Jun. 1967. [Online]. Available: http://en.wikipedia.org/wiki/Welch_method

[16] J. Sztajzel, "Heart rate variability: a noninvasive electrocardiographic method to measure the autonomic nervous system," *Swiss Medical Weekly*, vol. 134, 2004.

[17] M. Brennan, M. Palaniswami, and P. Kamen, "Do existing measures of poincarÃ© plot geometry reflect nonlinear features of heart rate variability?" *TRANSACTIONS ON BIOMEDICAL ENGINEERING*, vol. 48, no. 11, pp. 1342 – 1347, Nov. 2001. [Online]. Available: https://webvpn.uc.pt/http/0/ieeexplore. ieee.org/stamp/stamp.jsp?arnumber=00959330

[18] Y. Gang and M. Malik, "Heart rate variability analysis in general medicine," *Indian Pacing and Electrophysiology Journal*, vol. 3, no. 1, p. 34, 2003.

[19] E. L. Fallen, "Clinical utility of heart rate variability," *Cardiac Electrophysiology Review*, vol. 1, no. 3, 1997.

[20] J. Nolan, P. D. Batin, R. Andrews, S. J. Lindsay, P. Brooksby, M. Mullen, W. Baig, A. D. Flapan, A. Cowley, R. J. Prescott *et al.*, "Prospective study of heart rate variability and mortality in chronic heart failure: results of the united kingdom heart failure evaluation and assessment of risk trial (UK-heart)," *Circulation*, vol. 98, no. 15, p. 1510, 1998.

[21] PLUX, "bioPLUX research," www.plux.info. [Online]. Available: www.plux.info

[22] G. Lu and F. Yang, "Limitations of oximetry to measure heart rate variability measures," *Cardiovascular Engineering*, vol. 9, no. 3, pp. 119–125, 2009. [Online]. Available: http://www.springerlink.com/index/10.1007/s10558-009-9082-3

[23] S. Lu, H. Zhao, K. Ju, K. Shin, M. Lee, K. Shelley, and K. H. Chon, "Can photoplethysmography variability serve as an alternative approach to obtain heart rate variability information?" *Journal of Clinical Monitoring and Computing*, vol. 22, no. 1, pp. 23–29, 2007. [Online]. Available: http://www.springerlink.com/index/10.1007/s10877-007-9103-y

[24] J. Allen, "Photoplethysmography and its application in clinical physiological measurement," *Physiological measurement*, vol. 28, Feb. 2007. [Online]. Available: http://www.o2view.com/downloads/photoplethysmographyanditsapplicationinclinica.pdf

[25] E. Peper, R. Harvey, I. Lin, and H. Tylova, "Is there more to blood volume pulse than heart rate variability, espiratory sinus arrhythmia, and cardiorespiratory synchrony?" *Biofeedback*, vol. 35, no. 2, pp. 54–61, 2007. [Online]. Available: http://www.aapb.org/tl_files/AAPB/files/biof_35_2_blood.pdf

[26] A. Reisner, P. Shaltis, D. McCombie, and H. H. Asada, "Utility of the photoplethysmogram in circulatory monitoring," *Anesthesiology*, vol. 108, no. 5, pp. 950–958, May 2008. [Online]. Available: http://journals.lww.com/anesthesiology/Fulltext/2008/05000/Utility_of_the_Photoplethysmogram_in_Circulatory.24.aspx

[27] G. B. Moody, "PhysioNet RR/HR/HRV howto," http://www.physionet.org/tutorials/hrv/, 2009. [Online]. Available: http://www.physionet.org/tutorials/hrv/

[28] B. Analysis and M. I. Group, "Kubios HRV," http://kubios.uku.fi/, 2009. [Online]. Available: http://kubios.uku.fi/

[29] "Python programming language - official website," http://www.python.org/. [Online]. Available: http://www.python.org/

[30] T. M. Inc., "MATLAB." [Online]. Available: http://www.mathworks.com/products/matlab/

[31] N. community, *NumPy User Guide*, Aug. 2009. [Online]. Available: http://docs.scipy.org/doc/numpy/numpy-user.pdf

[32] S. community, *SciPy Reference Guide*, Mar. 2009. [Online]. Available: http://docs.scipy.org/doc/scipy/scipy-ref.pdf

[33] D. Dale, M. Droettboom, E. Firing, and J. Hunter, *Matplotlib*, Sep. 2009.

[34] "How to learn wxPython - wxPyWiki," http://wiki.wxpython.org/How to Learn wxPython. [Online]. Available: http://wiki.wxpython.org/HowtoLearnwxPython

[35] "Data acquisition systems | data loggers, amplifiers, transducers, electrodes for life sciences research | BIOPAC," http://www.biopac.com/. [Online]. Available: http://www.biopac.com/

[36] G. Friesen, T. Jannett, M. Jadallah, S. Yates, S. Quint, and H. Nagle, "A comparison of the noise sensitivity of nine QRS detection algorithms," *IEEE Transactions on Biomedical Engineering*, vol. 37, no. 1, pp. 85–98, Jan. 1990. [Online]. Available: http://ieeexplore.ieee.org/Xplore/login.jsp?url=http%3A%2F%2Fieeexplore.ieee.org%2Fstamp%2Fstamp.jsp%3Ftp%3D%26arnumber%3D43620%26isnumber%3D1671&authDecision=-203

[37] J. Pan and W. J. Tompkins, "A real-time QRS detection algorithm," *IEEE Transactions on Bio-Medical Engineering*, vol. 32, no. 3, pp. 230–236, Mar. 1985, PMID: 3997178. [Online]. Available: http://www.ncbi.nlm.nih.gov/pubmed/3997178

[38] W. Zong, T. Heldt, G. Moody, and R. Mark, "An open-source algorithm to detect onset of arterial blood pressure pulses," *Computers in Cardiology*, vol. 30, pp. 259–262, 2003. [Online]. Available: http://www.cinc.org/archives/2003/pdf/259.pdf

[39] K. M. V. and F. E. L., "Correction of the heart rate variability signal for ectopics and missing beats," in *Heart Rate Variability*.   Futura Pub. Co., 1995, pp. 75–85.

[40] R. Martins, "Desenvolvimento de um sensor de fotopletismografia para monitorização cardiaca para aplicação no pulso," 2010.

[41] D. G. Altman and J. M. Bland, "Measurement in medicine: the analysis of method comparison studies," *The statistician*, vol. 32, no. 3, pp. 307–317, 1983.

[42] J. M. Bland and D. G. Altman, "Statistical methods for assessing agreement between two methods of clinical measurement," *The Lancet*, vol. 327, no. 8476, pp. 307–310, 1986.

[43] J. Niskanen, M. P. Tarvainen, P. O. Ranta-Aho, and P. A. Karjalainen, "Software for advanced HRV analysis," *Computer Methods and Programs in Biomedicine*, vol. 76, no. 1, pp. 73–81, Oct. 2004, PMID: 15313543. [Online]. Available: http://www.ncbi.nlm.nih.gov/pubmed/15313543